Review

Fluorescence spectroscopy of rhodopsins: Insights and approaches ☆

CrossMark

Ulrike Alexiev [a,*], David L. Farrens [b]

[a] Physics Department, Freie Universität Berlin, Berlin, Germany
[b] Departments of Biochemistry and Molecular Biology, Oregon Health Sciences University, USA

ARTICLE INFO

ABSTRACT

Fluorescence spectroscopy has become an established tool at the interface of biology, chemistry and physics because of its exquisite sensitivity and recent technical advancements. However, rhodopsin proteins present the fluorescence spectroscopist with a unique set of challenges and opportunities due to the presence of the light-sensitive retinal chromophore. This review briefly summarizes some approaches that have successfully met these challenges and the novel insights they have yielded about rhodopsin structure and function. We start with a brief overview of fluorescence fundamentals and experimental methodologies, followed by more specific discussions of technical challenges rhodopsin proteins present to fluorescence studies. Finally, we end by discussing some of the unique insights that have been gained specifically about visual rhodopsin and its interactions with affiliate proteins through the use of fluorescence spectroscopy. This article is part of a Special Issue entitled: Retinal Proteins — You can teach an old dog new tricks.

1. Introduction

1.1. Overview of rhodopsins and rhodopsin photochemistry

Rhodopsins belong to the family of seven-transmembrane helix proteins that contain a retinal chromophore covalently linked to the apo-protein via a protonated Schiff base. This review will cover studies of two general categories of rhodopsins — microbial and visual. Their similarities and differences are briefly reviewed below.

Microbial rhodopsins are diverse in form and function, and include ion pumps, like bacteriorhodopsin (bR) and halorhodopsin [1–4], the archeal phototaxis receptors sensory rhodopsin I and II [5,6], and light-gated ion channels (channel-rhodopsins) that control photomovement of microalgae [7–9]. Upon excitation by light, the initial event in microbial rhodopsins is retinal isomerization from all-*trans* to 13-*cis*. This event triggers a cyclic reaction which involves Schiff base (SB) deprotonation, proton transfer steps, conformational changes of the protein, and the reversal of retinal isomerization. SB deprotonation results in a blue shifted intermediate that absorbs around 400 nm, and for most of the microbial rhodopsins this intermediate is called the M-state. This activation then leads to the specific function of the microbial rhodopsin in question.

In contrast, visual rhodopsins are much more similar and are focused on one goal — enabling the animal to "see" [10]. The visual rhodopsin molecules in vertebrate retinal photoreceptor cells are usually densely packed in the membranes of distinct disk-like organelles (disks). This high density of receptors and the dense stacking of the disks in the rod outer segments increase the ability of efficient photon capture. Visual rhodopsin acts as the primary light-sensing molecule triggering the signaling process that eventually converts a single photon into a visual response [11]. The chromophoric group of visual rhodopsin, 11-*cis* retinal, isomerizes to all-*trans* retinal upon light absorption [12]. The retinylidene chromophore is covalently bound to a conserved lysine residue (e.g. K296 in bovine rhodopsin) in transmembrane helix 7 (TM7). Interactions with amino acid residues in the surrounding binding pocket influence the absorption properties of retinal and control the photochemical pathways following light-activation. In the case of visual rhodopsin, SB deprotonation results in the formation of the metarhodopsin-II (MII) intermediate that absorbs at 380 nm. Subsequent hydrolysis of the SB leads to the release of all-*trans* retinal and the formation of opsin [13]. Visual rhodopsin belongs to the large class of G-protein coupled receptors (GPCR). MII activates a number of transducins (the cognate G-protein of visual rhodopsin), inducing them to take up GTP (guanosine triphosphate), and then to stimulate a cyclic guanosine monophosphate (cGMP) phosphodiesterase to hydrolyze cGMP. This results in closure of cation conduction channels in the cell membrane and the generation of a nerve signal.

1.2. Overview of the use of fluorescence to study rhodopsins

The use of fluorescence spectroscopy for investigating the structure and function of rhodopsin has a long history with initial work focusing primarily on the fluorescence properties of the bound cofactor retinal. Although rhodopsin itself is not detectably fluorescent due to the low quantum yield of retinal (e.g. 10^{-5} for visual rhodopsin), fluorescence

emission from some of the intermediates of the vertebrate visual cycle has been reported [14,15]. The first FRET (Förster resonance energy transfer) studies on rhodopsin labeled with organic dyes were conducted as early as 1972 [16].

Most recent studies of retinal proteins (and its various affiliate proteins) have followed the approach pioneered by those early FRET studies, although the fluorescence of intrinsic tryptophan residues has also been exploited. These studies have provided unique insights into questions of protein dynamics, conformational changes, photocycle kinetics and protein–protein interactions. New advancements in fluorescence techniques [17–19] have facilitated several of these works. Here, we will review and discuss some of the unique insights gained and challenges faced when studying retinal proteins by fluorescence spectroscopy.

2. Basic concepts of fluorescence

Below we provide a brief review of fluorescence theory, concepts and terminology, before discussing the specific applications to retinal proteins.

2.1. Jablonski diagram

Essentially, one can think of fluorescence as simply the inverse process to absorption. After the initial absorption of a photon by a fluorophore in accordance with the Franck–Condon principle, a non-radiative relaxation to the lowest excited energy state takes place. For this reason, the emission of a photon occurs from the first excited state with the lowest vibrational quantum number. This is in general the S_1 state (or the T_1 state) of a molecule (Fig. 1A). The emission of a photon during the transition from the excited energy state (S_1) to the lower electronic energy state (S_0) is called fluorescence. Because a number of events occur before an excited electron can return to the ground state by emitting a photon, fluorescence is usually observed to take place on the pico- to nanosecond time scale. Depending on the electronic structure of the molecule, fluorescence occurs for

Fig. 1. (A) Jablonski diagram illustrating possible electronic states of a fluorophore and the energy transitions in this molecule: absorption in blue, emission in red, vibrational relaxation and internal conversion in dashed blue and intersystem crossing/phosphorescence in gray. Singlet states are abbreviated as S and triplet states as T. The spin states are also given. (B) Absorption and emission spectra of tryptophan. Fluorescence excitation was at 280 nm.

most fluorophores within 1–100 ns. Besides absorption, dissipation (vibrational relaxation and internal conversion) and fluorescence, spin–orbit-coupling can lead to spin–flip intersystem crossing and long-lifetime phosphorescence. All four processes are illustrated in the Jablonski diagram shown in Fig. 1A.

2.2. Fluorescence properties (fluorescence intensity, quantum yield and lifetime)

Since the emitting state is the lowest vibrational level of the S_1 state, the fluorescence spectrum is usually shifted to lower energy, i.e. to higher wavelengths compared to the corresponding absorption spectrum. This so-called Stokes shift is clearly visible in the absorption and emission spectra of tryptophan, shown in Fig. 1B.

How "fluorescent" a given fluorophore is depends on how efficiently it can convert absorbed photons back into emitted light, i.e. how many photons come out compared to how many went in. This value, called the quantum yield η, is described as:

$$\eta = \frac{\text{number of emitted photons}}{\text{number of absorbed photons}}. \tag{1}$$

In the absence of any non-radiative processes the quantum yield of a molecule is thus 1. Any molecular mechanism leading to a non-radiative depopulation of the excited state reduces the quantum yield.

The fluorescence lifetime τ is the average time that the fluorophore spends in the excited state before emitting a photon. Both emission and non-radiative relaxations to the electronic ground state are the main processes that determine the lifetime. Using the emissive rate constant (k_r) and the rate constant for all non-radiative relaxations (k_{nr}), the above introduced quantum yield can be rewritten as:

$$\eta = \frac{k_r}{k_r + k_{nr}}. \tag{2}$$

The fluorescence lifetime τ is the inverse of all rate constants describing the depopulation of the excited state:

$$\tau = \frac{1}{k_r + k_{nr}}. \tag{3}$$

The average fluorescence intensity I as a function of time t of a single fluorophore species is proportional to the population of excited molecules generated at the moment of excitation, which starts to decay exponentially through the radiative and non-radiative transitions to the ground state:

$$I(t) = I_0 \exp(-t/\tau). \tag{4}$$

Environmental properties are known to strongly affect both spectral and lifetime values, as well as the quantum yield [18].

2.3. Fluorescence quenching and energy transfer mechanisms

2.3.1. Fluorescence quenching

A molecule that interacts with the fluorophore and reduces its quantum yield or lifetime is called a quencher. The process of fluorescence quenching can be further resolved into two different types, dynamic and static quenching [18,20]. In the case of dynamic quenching the quencher molecule collides with the fluorophore in the excited state. Since such an event represents an additional way of depopulating the excited state, it thus affects the rate of fluorescence decay (Fig. 2B). For static quenching, the fluorophore and the quencher form a non-fluorescent complex, with the number of these complexes tending to increase with increasing concentration of quencher molecules. Interestingly, the non-fluorescent complexes formed in static quenching reduce the observed steady-state fluorescence yield (Fig. 2A), but have no effect on the
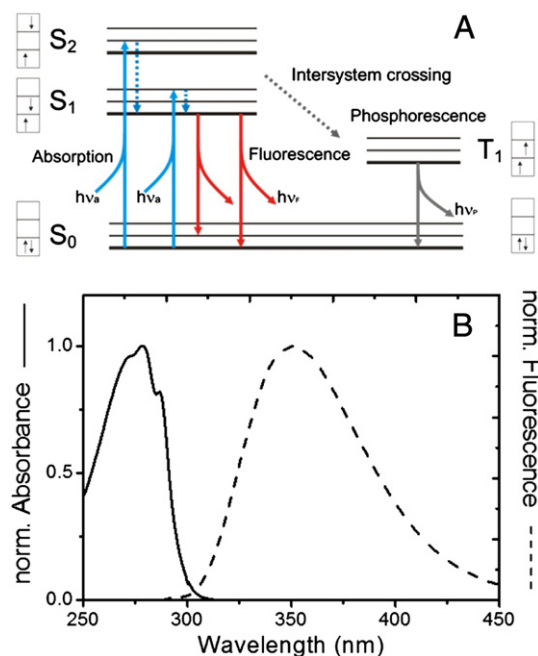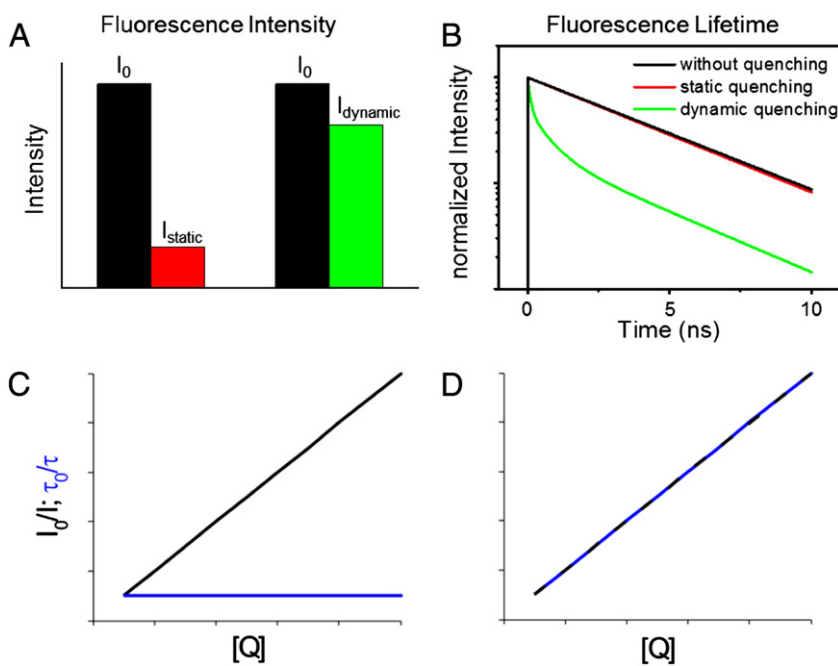
Fig. 2. Differences in static and dynamic quenching as evidenced by steady-state (A) and time-resolved fluorescence (B). Stern–Vollmer plots showing (C) static and (D) dynamic quenching.

fluorescence decay rates for the remaining non-complexed molecules (Fig. 2B). Fig. 2C and D depicts the Stern–Volmer plots describing static and dynamic quenching for both steady-state (black curve) and time-resolved (blue curve) fluorescence yield.

2.3.2. Electron transfer based quenching mechanisms

Long and short range energy transfer mechanisms also lead to a depopulation of the excited state. Short range energy transfer (within distances up to ~1 nm) is mediated by electron transfer between a fluorophore and quencher that can occur when the two molecules come in contact. Several different mechanisms of electron transfer induced quenching are known, including Dexter mechanism [21] and photo-induced electron transfer [22]. For these types of quenching, the rate of energy transfer is proportional to the decay of the electron density of the electron shells, thus the quenching efficiency is determined by the ratio of the interaction rate and the emissive rate from the excited state. Essentially, the extent of quenching depends on whether or not the rate of electron transfer is greater than the rate of fluorescence decay. If the fluorescence decay rate is faster than electron transfer, no quenching is observed. For these reasons and others, electron transfer quenching mechanisms are usually only effective over very short distances. In the case of photo-induced electron transfer, a redox reaction (electron exchange) takes place after formation of the donor–acceptor complex with the fluorophore being in its excited state. Whether the fluorophore or the quencher acts as a donor in the complex depends on the redox potentials of the quencher and fluorophore in the excited state.

A fluorophore and quencher pair widely used in protein fluorescence spectroscopy is an organic fluorophore together with the amino acid tryptophan (Trp) acting as the quenching agent [23,24] (for further discussion see Sections 5 and 6). A key advantage in this type of quenching experiments is that only one extrinsic fluorophore has to be covalently linked to the protein, while the quencher (Trp) is present in the protein sequence. Fig. 3 depicts the various possible scenarios in the tryptophan quenching studies. The amount of dynamic and static quenching can be quantified to gain insights into the distribution of fluorophore–quencher pairs. Specific distance information in the range up to 1 nm, distances that are usually too small to be discriminated by FRET approaches (see below), is thus available from the experiments.

As shown in Fig. 3, by simply comparing changes in fluorescence emission intensity with changes in the fluorescence lifetime one can determine if the fluorescent probe is in contact with a tryptophan at the moment of light excitation. At larger separation distances, probes can be described as being in an "open" state; that is, they are not in contact with the tryptophan before light excitation. The fraction of these "open" probes that never interact with the tryptophan will thus exhibit maximal fluorescence (Fig. 3 I, illustrated as "unquenched"). Some "open" probes that are closer can interact with the tryptophan at some time after excitation, and will thus undergo "dynamic quenching" (Fig. 3 II). A population of dynamically quenched probes will exhibit decreased fluorescence intensities and lifetimes, with the magnitude of decrease dependent on the amount of interaction. Of special interest are probes that are very close to the tryptophan, even before light excitation. If these probes contact the tryptophan and form a nonfluorescent complex (indicated as "complexed") they undergo what is called "static quenching" (Fig. 3 III) and thus do not contribute to the emission intensity or lifetime. In most cases both scenarios are present, i.e. mixtures of "open" and "complexed" probes exist (Fig. 3 IV and V). Here the relative fraction of probes in the respective state can be determined from analysis of the fluorescence data. The fraction of probes in the open state, called f_o, is readily extracted from the fluorescence data using the relationship indicated in Fig. 3. In essence, this relationship is the ratio of the fluorescence intensities in the presence (I_W) and in the absence of tryptophan (I_0), normalized by the respective lifetimes (τ_W and τ_0) of the fluorescent probe. In turn, the relative fraction of "complexed" probes is simply ($1 - f_o$).

2.3.3. Fluorescence resonance energy transfer (FRET)

Fluorescence energy transfer over longer distances is described by the quantitative theory for resonance energy transfer, also known as Förster
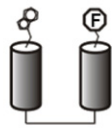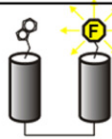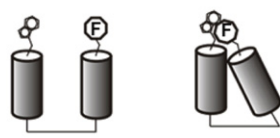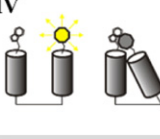
ground state	after light excitation

Fig. 3. Fluorescence characteristics in tryptophan induced quenching experiments (called TrIQ experiments in [24]) and distance information provided by comparing fluorescence intensity and lifetime.

resonance energy transfer (FRET) [25]. FRET is a dipole–dipole interaction mediated energy transfer between two molecules, the donor (D) and the acceptor (A) molecule, at a certain distance (Fig. 4A). Spectral overlap between the donor fluorescence and the acceptor absorption band is required to transfer the excited state energy of the donor non-radiatively to the acceptor molecule in the ground state (Fig. 4B). FRET is highly sensitive for measuring distances since the rate constant of energy transfer is proportional to the inverse 6th power of the distance. Fig. 4A illustrates the dependence of FRET efficiency on the distance (R) between the donor and acceptor, and the Förster distance R_0. R_0 is the critical distance

Fig. 4. FRET concept. A) Distance dependence of FRET efficiency, B) overlap of donor emission and acceptor absorption, and C) shortening of donor fluorophore lifetime in the presence of a FRET acceptor.

at which the excitation energy of the donor is transferred to the acceptor with a probability of 0.5 (Fig. 4A). Typical FRET distances are between 1 and 10 nm. The energy transfer efficiency E is:

$$E = \frac{1}{1 + (R/R_0)^6}. \tag{5}$$
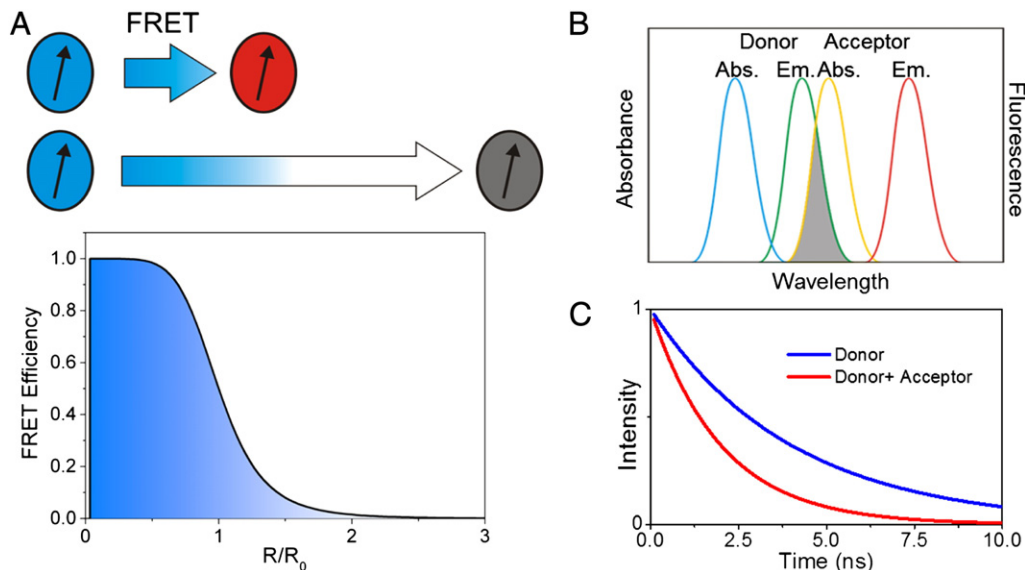
The Förster distance (in Å) can be calculated from the spectroscopic parameters and mutual dipole–dipole orientation of donor and acceptor:

$$R_0 = 0.211 \left[\kappa^2 Q_D n^{-4} J \right]^{1/6} \tag{6}$$

with κ^2 the orientation factor, Q_D the quantum yield of donor fluorescence (without acceptor), and n the refractive index of the medium. J (in M^{-1} cm^{-1} nm^4) is the spectral overlap integral of donor fluorescence and acceptor absorption. The dipole orientation factor κ^2 assumes a value of 2/3 when dynamical reorientation of the dyes results in orientational averaging. If, however, the dipoles of a donor–acceptor pair adopt a particular orientation to each other, e.g. when the donor is restricted through interactions with the membrane and the acceptor is rigidly bound to the membrane protein core (such as the chromophore retinal), the deviation of the orientation factor from its dynamically averaged value needs to be considered. Time-resolved fluorescence anisotropy experiments (see below) provide an approach to evaluate the dynamical reorientation of the fluorescent dyes.

Quantification of FRET efficiency by the shortening of the donor fluorescence lifetime in the presence of the acceptor (Fig. 4C) is a reliable method since the fluorescence lifetime is a concentration independent parameter. FRET efficiency based on fluorescence lifetime can be calculated by:

$$E = 1 - \frac{\tau_{DA}}{\tau_D} \tag{7}$$

with τ_D the lifetime of the unquenched donor and τ_{DA} the lifetime of the donor in the presence of the acceptor.

2.4. Fluorescence anisotropy

The basic principle of time-resolved fluorescence anisotropy relies on the excitation of dye molecules in solution by a short polarized laser pulse resulting in photoselection of those dye molecules having their absorption transition dipole moments oriented along the direction of the electric field vector of the polarized exciting light (Fig. 5C). After a period of time t, during which the dye has undergone rotational diffusion, the polarization of the emitted light is measured as the parallel ($I_{II}(t)$) and perpendicular ($I_\perp(t)$) fluorescence intensities with respect to the field vector of the exciting light pulse (Fig. 5A and C). Rotational diffusion changes the direction of transition dipole moments and the anisotropy measurement reveals the angular displacement of the chromophore that occurs between absorption and emission of a photon. The fluorescence anisotropy $r(t)$ at time t after excitation of the fluorophore (Fig. 5B) is defined as

$$r(t) = \frac{I_{II}(t) - I_\perp(t)}{I_{II}(t) + 2I_\perp(t)}. \tag{8}$$

The angular displacement is dependent on the rate and extent of rotational diffusion. The decay of the time-resolved anisotropy is commonly described with an exponential decay model function yielding a decay time constant or rotational correlation time ϕ, which is determined by the rotational diffusion coefficient. Fig. 5B (green curve) illustrates the rotational diffusion of the fluorescent dye fluorescein free in aqueous solution, where the anisotropy shows a mono-exponential decay to zero. When the fluorescent dye has been covalently attached to the protein (Fig. 5D), the motional freedom of the dye, i.e. the extent of rotational diffusion, is restricted due to interactions with the surrounding protein constituents. In addition, rotational diffusion may occur not only because of the tumbling motion of the whole molecule but also because of the (faster) motion of the protein segment to which the fluorescent dye is attached [26]. Thus, the orientational dynamics of the fluorescent dye
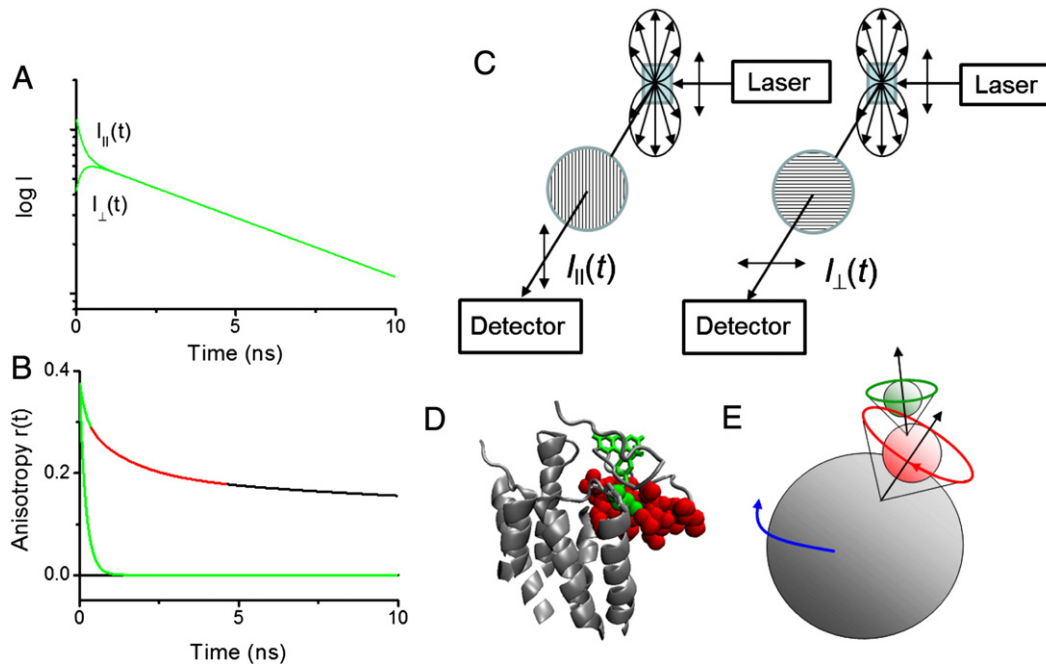
Fig. 5. Anisotropy concept. (A) Time courses of the fluorescence intensities $I_{II}(t)$ and $I_\perp(t)$. (B) Corresponding fluorescence anisotropy decay. Green curve — fluorescent dye free in solution. Upper curve — anisotropy decay of a fluorophore bound to a protein surface segment (see (D)). The different colors indicate the main anisotropy decay components resulting from rotational diffusion of the bound fluorophore (green), the segmental mobility (red) and the rotation of the whole protein (black). (C) Scheme of measurement principle. (D) Structural model of bovine rhodopsin (PDB ID: 1U19) with fluorescein (green) covalently bound to Cys316 in H8 (red). (E) The schematic visualizes how protein dynamics is described by the protein segment cone (here H8, red), within which the dye cone (green) freely diffuses [29]. Color coding corresponds to the colors used in (B) and (D).

is also affected by the local flexibility of the protein and the bound dye can serve as a probe for protein flexibility and conformational dynamics. As a consequence, we will measure a time course of fluorescence depolarization $r(t)$ for the attached fluorescent probe that exhibits a multi-exponential anisotropy decay (Fig. 5B, upper curve):

$$r(t) = \sum_{i=1}^{n} \beta_i e^{-t/\phi_i} \qquad (9)$$

with β_i the amplitude and ϕ_i the correlation time of the ith decay component, and the initial anisotropy $r_0 = \sum_{i=1}^{n} \beta_i$. If the rotational correlation time of the last decay component is much slower than the lifetime of the fluorescent probe ($\phi_n \gg \tau$), such as for rhodopsin in disk membranes or bR in purple membrane fragments with a rotational correlation time of the membrane fragment in the milliseconds time range, then the anisotropy decays virtually to a constant end value r_∞ in the ns time range of the measurements that is determined by the lifetime of the fluorescent probe [26]. The value of r_∞ or β_n represents a measure of the degree of steric hindrance by the protein surface. The relation between ϕ and τ is illustrated by the Perrin equation:

$$r_0/r = 1 + (\tau/\phi) \qquad (10)$$

i.e. when $\phi \gg \tau$ the observed anisotropy r is equal to the initial anisotropy r_0 for a mono-exponential anisotropy decay, or in our case when $\phi_n \gg \tau$ the observed anisotropy is equal to the amplitude $\beta_n = r_\infty$. The amplitudes β of the decay components, which reflect the extent of the rotational diffusion for a given anisotropy decay component, can be used as a measure of the conformational space for that motion. A small amplitude β reflects a small conformational space and a high steric restriction by the surrounding protein constituents (Fig. 5B, D, and E). A common model to describe restricted rotational diffusion is the "wobbling-in-a-cone" model [27]. In this model, the transition dipole is assumed to diffuse freely inside a cone, fixed within the molecular frame. Extension of this model for the local flexibility of proteins, which affects cone orientation and possibly cone angle (Fig. 5E), leads to the "cone-in-a-cone" model [28]. Thus, the anisotropy decay curve

yields information on global and local protein dynamics as well as on the protein structure and conformational changes.

Rotational diffusion depends on the size and shape of the rotating molecule as well as on the viscosity of the solvent (Fig. 5E; [29]), and these parameters can be extracted using the following relation (here given for a spherical rotator):

$$\phi = \frac{\eta V}{k_B T} \qquad (11)$$

with V the apparent volume of the molecule, η the viscosity, T the temperature, and k_B the Boltzmann constant.

3. Fluorescence probes used in studies of rhodopsin

3.1. Intrinsic probes in rhodopsins — retinal

Bound retinal (Fig. 6) by itself is only weakly fluorescent due to its low quantum yield. The low quantum yield of retinal corresponds to the extremely fast return to the ground state after retinal excitation that is in the low picosecond to femtoseconds range [30]. Quantum yield values of 1–3×10^{-4} were found for 13-*cis* and all-*trans*-retinal in bacteriorhodopsin [31]. Similar low quantum yields of about 10^{-5} for retinal in visual rhodopsin [32], and 2.6×10^{-4} in proteorhodopsin were determined [33]. Weak fluorescent states in the near-infrared regions were reported for several microbial rhodopsins (see below) as well as for visual rhodopsin [14,15].

An exciting new field in biological fluorescence involves the generation of better fluorescent proteins (FPs) for optogenetic tools. These new developments include rhodopsin-based FPs. Two engineered microbial rhodopsin-based voltage-sensitive FPs were recently reported, a proteorhodopsin-based optical proton sensor (PROPS) [34] and archaerhodopsin3 [35]. These voltage-sensitive FPs allow for the optical recording of membrane potential thus providing a new tool to gain insights into the dynamics of physiological important processes, such as in neurons, cardiac cells or developing embryos. In both cases the microbial rhodopsins were weakly fluorescent in the photocycle ground state. In proteorhodopsin, a mutation (D97N) generated a non-proton pumping variant that shifted the pK_a of the SB in a physiological pH
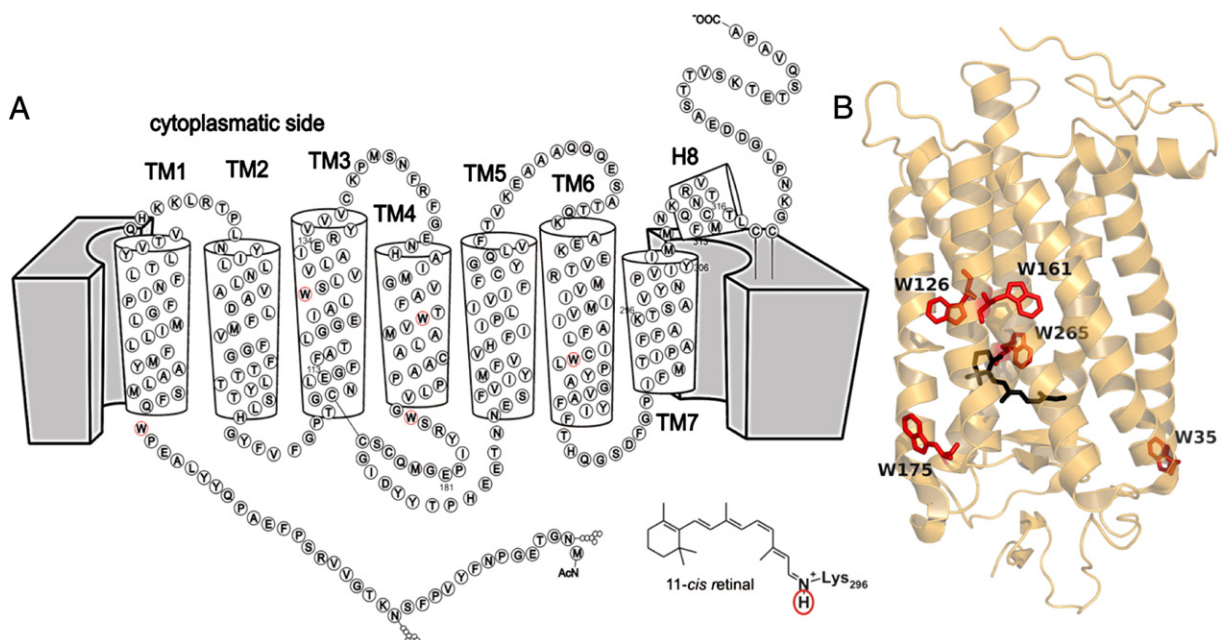

Fig. 6. Secondary (A) and tertiary (B) structural model of bovine rhodopsin (PDB ID: 1U19). Tryptophan residues (red) and retinal (black) are highlighted.

range. Weak fluorescence in the near infrared occurred from the protonated SB species while the deprotonated species remained nonfluorescent [36,37]. This phenomenon – the increase of excited state (fluorescence) lifetime and thus the fluorescence intensity upon protonation of the SB counter ion at low pH or its neutralization by the respective mutant (D85N) – was already observed earlier for bR [31,38,39]. Modulation of the membrane potential was shown to alter the acid-base equilibrium of the SB, thus proving it possible to correlate the proteorhodopsin fluorescence with the membrane voltage. The corresponding mutation in archaerhodopsin3 (D95N) generated a variant with an even higher fluorescence voltage sensitivity compared to wild type [35]. Further archaerhodopsin3 photocycle analysis revealed that a three photon process (initiation of photocycle, formation of a fluorescent species of an intermediate photocycle state, excitation of this fluorescent species) generates a photocycle-derived 13-*cis* retinal containing intermediate with high fluorescence [40]. It has to be noted, however, that such a three photon process is very unlikely to occur. This may complicate the general applicability of archaerhodopsin3 as a potential sensor.

Another way to generate fluorescent retinal proteins has been to increase the excited state lifetime of the retinal in non-fluorescent rhodopsins using appropriate retinal analogs [41]. One extreme way to achieve this is to prevent the fast isomerization process that normally would consume most of the energy. In experiments employing this approach, retinal with an 85 ps lifetime with no photoproduct formation has been observed [42].

It is also possible to create fluorescent retinal proteins using chemical (NaBH$_4$) reduction of the retinal SB linkage. This approach yields a fluorescent retinal, N-retinyl-opsin, both for bacteriorhodopsin [43] and visual rhodopsin [44,45]. Reduction of the retinal SB linkage may also be achieved by two-photon excitation [46], where the two-photon photoreduction results in similar photoproducts as for chemical reduction with peaks at 340 nm, 360 nm, and 380 nm.

3.2. Intrinsic probes in rhodopsins — tryptophan

Most retinal proteins contain between 5 and 13 tryptophan residues in their sequence. For example, bovine visual rhodopsin (shown in Fig. 6) has five tryptophan residues. Because these tryptophans are mainly located near to the retinal chromophore in the three-dimensional protein structure, their fluorescence is quenched (decreased) due to very efficient energy transfer to the retinal. Tryptophan fluorescence and its use as an internal indicator are further discussed in Sections 4.1. and 5.1.

3.3. Extrinsic fluorescent probes — biosynthetically attached fluorescent proteins

Green fluorescent protein (GFP) fusions provide a convenient and unique way to tag the protein of interest in a cellular or living animal context [47]. GFP tagging and visualization have been carried out in a number of rhodopsin studies. Such work includes the studies of channelrhodopsin in single *Caenorhabditis elegans* neurons [48], monitoring the degradation and mislocalization of the human retinitis pigmentosas rhodopsin variant P23H-rhodopsin-GFP in knockin mouse models [49], FRET studies of rhodopsin aggregation in COS-1 cells (using cyan and yellow variants of GFP fused to the C terminus of visual rhodopsin) [50], and investigations into the stoichiometry of rhodopsin interactions with transducin [51]. Although a powerful approach, GFP tagging does have some caveats. For example, when interpreting GFP tagging data it is important to take into account the large size of the tag (GFP is almost as large as the rhodopsin itself), to ensure rhodopsin function has not been affected.

3.4. Extrinsic fluorescent probes — covalently attached synthetic molecules

A typical approach for labeling of proteins with extrinsic fluorescent probes is to use the reactive thiol-group of cysteine residues as a specific attachment site for organic dyes [52]. This approach has been used extensively in studies of rhodopsins [3,16,28,29,52–64]. Fluorescent dyes that are derivatized by a thiol-reactive linker for coupling to the cysteines include small probes like bimane, but also larger fluorophores such as Lucifer Yellow, fluorescein, tetramethylrhodamine or Alexa dyes, just to name a few. Although other groups besides thiols can also be targeted, for example amino groups [65], the use of single cysteine residues is still the primary approach employed in site-directed fluorescence labeling (SDFL) strategies, as discussed later in Section 5.2.

One drawback with relying on cysteines to attach fluorescent dyes is that it often requires the researcher to carry out extensive mutagenesis of the protein in order to remove reactive "background" cysteines, before the cysteine of interest can be introduced. Moreover, these substitutions can sometimes affect protein folding and function. Recently, an alternative and efficient site specific labeling technique that avoids these issues was developed for seven helix transmembrane proteins based on unnatural amino acids mutagenesis [66]. The technique was applied to visual rhodopsin as a model receptor and yielded functional proteins expressed in mammalian cells. The unique reactive keto group, which is provided by the incorporated unnatural amino acids *p*-acetyl-L-phenylalanine and *p*-benzoyl-L-phenylalanine, reacts highly specific with hydrazide or hydroxylamine derivatives, allowing for site-specific labeling. Successful labeling with fluorescein hydrazide at the extracellular side of rhodopsin was shown *in vitro* [67].

4. Challenges in performing fluorescence experiments with retinal proteins

A number of unique issues must be taken into account when carrying out fluorescence studies of retinal proteins. Three of these issues – FRET effects from the fluorophore to the retinal, retinal bleaching by the fluorescence excitation light, and effects caused by high rhodopsin concentrations in membranes – are briefly discussed below.

4.1. Quenching of fluorescence due to energy transfer to the bound retinal

Retinal proteins, by definition, contain an intrinsic chromophore (retinal), which has an absorption spectrum that overlaps with the fluorescence emission of tyrosine and tryptophan, as well as with the fluorescence emission of most extrinsic fluorophores. The issue of FRET from intrinsic chromophores to retinal is illustrated in Fig. 7A, which shows both the overlap in absorbance of all-*trans* (in MII) and 11-*cis* retinal (in the dark-state (DS)) with tryptophan emission. Fig. 7B shows an example of overlap between an extrinsic fluorophore (in this case bimane) and retinal. The overlap with bimane is substantially decreased for the MII state, resulting in less energy transfer, and a concomitant increase in bimane emission [52,57].

Thus, the issue of FRET from both internal and external fluorophores is substantial and must be taken into account. In fact, FRET to retinal can even be exploited for analysis, as is discussed further in Section 5. One unique aspect of rhodopsin fluorescence studies involves the fact that during the light-activated photocycle, with the corresponding changes in retinal absorption, the amount of FRET will change at each step (since the retinal changes its absorbance while traversing through the photocycle). Such photochromic FRET changes as well as concomitantly occurring intensity changes due to environmental effects on the fluorescent probe have to be taken into account when interpreting changes in exogeneous fluorophore intensity during the photocycle in terms of rhodopsin photocycle intermediate states [68,69] or conformational changes [70–72].

4.2. Visual rhodopsin — the bleaching effect

Another major concern when studying retinal proteins is that the very act of probing the fluorophore with excitation light can (and will) also cause some amount of photoactivation of the retinal. In the case of visual rhodopsin, this can result in bleaching of the sample (conversion of the
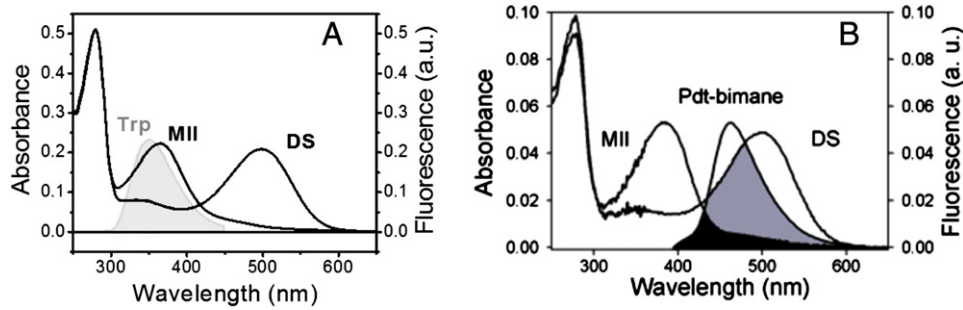
Fig. 7. Example of spectral overlap of a fluorophore emission (A — Trp, B — bimane) with retinal absorption in rhodopsin dark state (DS) and MII. In the case of the exogeneous fluorophore there is more overlap of the bimane fluorescence emission spectrum with dark state (DS) rhodopsin (shaded gray and black) than with MII rhodopsin (black only), and thus more energy transfer from the bimane to retinal.

dark-state chromophore with absorbance maximum at 500 nm to the active MII state with absorbance maximum at 380 nm, see Fig. 7). Thus, when carrying out fluorescence studies of rhodopsins it is critical to maximize capture of the emitted light, while at the same time using the least amount of excitation light as possible in order to minimize the amount of photobleached retinal. In practical terms, this often means using very tight excitation slits and/or neutral density filters (on traditional fluorescence instruments) to achieve low excitation, and broad-band capture of emission. For example, in our laboratories, when carrying out studies of retinal release from bovine rhodopsin, the excitation slits will usually be set as small as possible (usually ~0.25 nm (bandpass) excitation slits), while maximizing the amount of captured emission, for example using >10 nm (bandpass) emission slits to reliably obtaining reasonable signal to noise ratios. In single photon counting detection schemes, in particular in time-resolved fluorescence experiments using time-correlated single photon counting (TCSPC) [26,71], a sufficient signal to noise ratio is obtained at very low intensities of excitation light that results in negligible bleaching of rhodopsin [26,71,73].

To be on the safe side, in particular when high excitation power is required such as in microscopy studies, it is always best to use fluorophores that exhibit absorbance maxima which are red shifted compared to the absorbance band of rhodopsin. Examples are fluorescent dyes such as

Atto647N, which can be excited at 640 nm where the amount of rhodopsin absorption is negligible [74]. Another approach is to constantly introduce new sample into the measuring beam.

4.3. Drawbacks of high retinal protein concentrations in membranes on fluorescence studies

Many rhodopsins exist in membranes at high concentrations. Fig. 8 shows examples of the high protein density and organization of rhodopsins in the purple (bR) and disk (visual rhodopsin) membranes. bR is organized as a trimer in a hexagonal lattice [75], whereas rhodopsin may adopt a paracristalline lattice arrangement (based on the model described in [76]).

In general, these high protein concentrations have greatly facilitated biophysical studies. However for fluorescence studies, in particular fluorescence anisotropy and FRET studies, the high densities can present unique challenges. The close proximity of the individual rhodopsins in the membrane has to be taken into account because homo-energy transfer between neighboring fluorescent probes may occur. This results in additional components in the fluorescence anisotropy decay. Therefore, the labeling stoichiometry (i.e. the amount of fluorophore per protein molecule, see Eq. (12)) is an important parameter. The
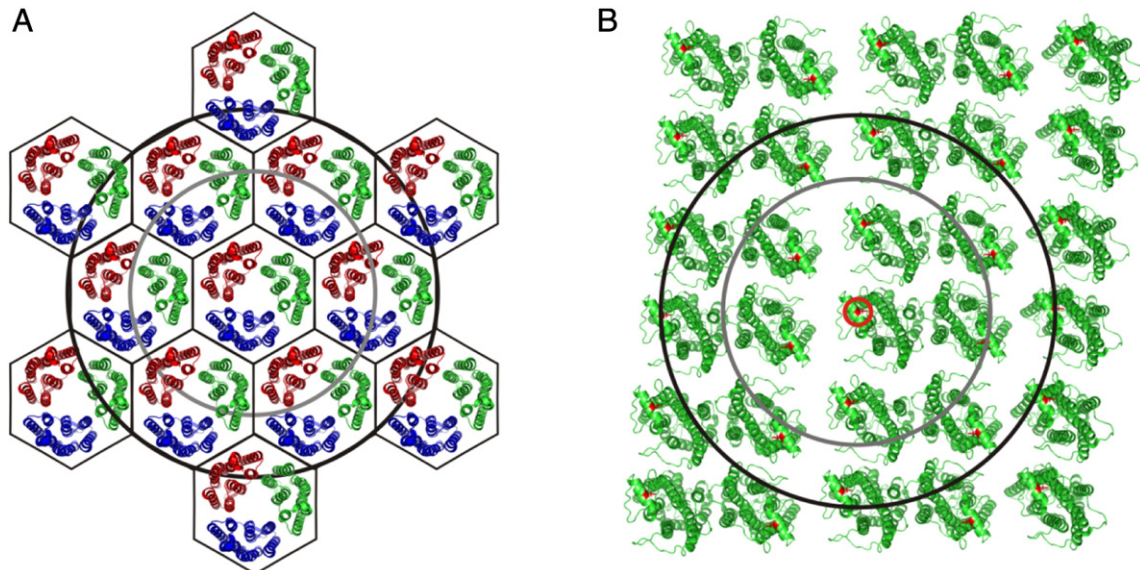

Fig. 8. Arrangement of (A) bacteriorhodopsin in purple membrane (PDB ID: 1C3W) and (B) possible paracristalline lattice organization of visual rhodopsin (PDB ID: 1N3M). Details are given in the text.

labeling stoichiometry needs to be reduced in order to prevent homo-energy transfer between nearby fluorescent probes. Let us assume we use fluorescein with a Förster distance of $R_0 = 44$ Å for homo-energy transfer. Eq. (5) allows us to calculate the distances and the corresponding energy transfer efficiencies. For 8% or 4% labeling stoichiometry, i.e. only one out of 12 or 27 bR molecules is labeled (indicated by the gray and black circles in Fig. 8A), we obtain a maximum theoretical energy transfer efficiency of 11% and 1%, respectively. In the case of visual rhodopsin, for a labeling stoichiometry of 17% or 7%, i.e. only one out of 6 or 14 rhodopsin molecules is labeled (indicated by the gray and black circles in Fig. 8B), we obtain a maximum theoretical energy transfer efficiency of 19% and 2%, respectively. In reality, the efficiencies may be less. According to experimental test measurements, no detectable contribution of homo-energy transfer was obtained using a labeling stoichiometry of about 10% for bR and 20% of rhodopsin [26,70]. Similar considerations have to be taken into account when setting up FRET experiments.

5. Experimental approaches to gain unique insight into rhodopsin structure and function

As shown in Fig. 9, a number of different fluorescence approaches can be (and have been) used to study the structure and dynamics of rhodopsin proteins. These are briefly reviewed below.

5.1. Tryptophan fluorescence as an internal indicator for retinal binding and release, protein folding, structural dynamics and conformational changes

In visual rhodopsin, the fluorescence of the five tryptophan residues is quenched by their close proximity to the retinal chromophore (Fig. 6). It was observed somewhat accidentally (Farrens, personal communication) that the tryptophan fluorescence of opsin increases as a function of time after photo-activation. This phenomenon was subsequently investigated and established to be due to release of retinal following SB hydrolysis, and an assay for retinal release was established that allows to follow MII decay [77]. Note that the phenomenon of increasing tryptophan fluorescence of rhodopsin after bleaching appears to have been observed in rhodopsin by investigators in the late 1960s and early

1970s [45,78], although the underlying mechanism was not completely clear at that time. A number of investigations have exploited this phenomenon to monitor the kinetics of retinal release, both in rhodopsin [79–81], and more recently in cone opsins [82,83]. Retinal binding can also be monitored in this way, essentially as the inverse of this process [84]. One caveat when carrying out retinal release or binding studies, especially in membranes, relates to the fact that if retinal concentrations are high enough, such that the relative retinal/protein ratio is very high, there is concern that significant decrease in tryptophan fluorescence may occur that is not related to retinal binding, but rather, is simply due to FRET from the tryptophan residues to excess retinal molecules located nearby in the membrane or micelle (see discussion above about challenges due to high protein concentrations).

Retinal binding and release are tightly connected to the folding and unfolding of rhodopsins. Unfolding and refolding studies using intrinsic fluorescence probes (Trp) were performed with bR [85,86] and visual rhodopsin [87,88] as models to study membrane protein folding. The kinetics of tryptophan fluorescence changes upon bR folding revealed discrete steps for retinal binding to an apoprotein intermediate state and for later formation of the covalent SB linkage, thus generating new insights into the folding pathway of bR [85]. To understand retinal protein folding (and membrane folding in general) information about residual structure in unfolded states of these proteins is mandatory. In this context, changes in tryptophan fluorescence made it possible to analyze how various concentrations of the denaturant SDS affect the tertiary structure and integrity of visual rhodopsin and revealed two different stages of unfolded structures at low and high concentrations of SDS, respectively [88].

To investigate the structural changes in the transmembrane part that occur upon transfer from the lipid membrane to SDS micelle environment, a two helix fragment comprising transmembrane helix A and B of bR was recently investigated by FRET [89]. The protein intrinsic tryptophan (helix A) and tyrosine (helix B) residues were utilized. Importantly, the study indicated that disappearance of FRET upon changing the environment does not necessarily indicate structural disruption, but may also be explained by changes in the photophysics of the fluorophores [89].

Since the bound retinal undergoes isomerization and thus changes its interactions with the binding pocket after light-activation, kinetic measurements of tryptophan fluorescence during the photocycle of rhodopsins are sensitive to structural dynamics and conformational changes that occur during the photocycle. Tryptophan fluorescence quenching was used as a monitor for protein conformation changes occurring during the photocycle of bR [90]. In particular, tryptophan fluorescence changes were observed upon formation of the M-intermediate [90]. A similar result was obtained in investigations of tryptophan fluorescence changes upon formation of the MII state in visual rhodopsin [69].

5.2. Fluorescence labels as reporter groups for molecular and cellular protein dynamics, conformational and environmental changes and protein interaction

As mentioned above, most work involving labeling of proteins with external fluorophores utilizes "Site-Directed Fluorescence Labeling", or SDFL. In SDFL, fluorescent probes are attached to the rhodopsins at specific sites in order to monitor protein conformation and dynamics, stoichiometry and protein–protein interactions [52]. Briefly, in SDFL studies mutagenesis is used to introduce individual cysteine residues into the region of interest in the protein. For this approach to work, it is also necessary to have a "background" protein sequence that contains no reactive cysteines (note this does not necessarily require removal of all cysteine residues, simply all reactive ones). Individual cysteines are then used as attachment sites for sulfhydryl-reactive fluorophores, followed by studies using the appropriate method as outlined in Fig. 9. Examples for each of the methods are given below in Sections 5.2.1–5.2.4.

When using fluorescently labeled proteins, the degree of labeling is an important issue. Low labeling stoichiometry can be used for all studies
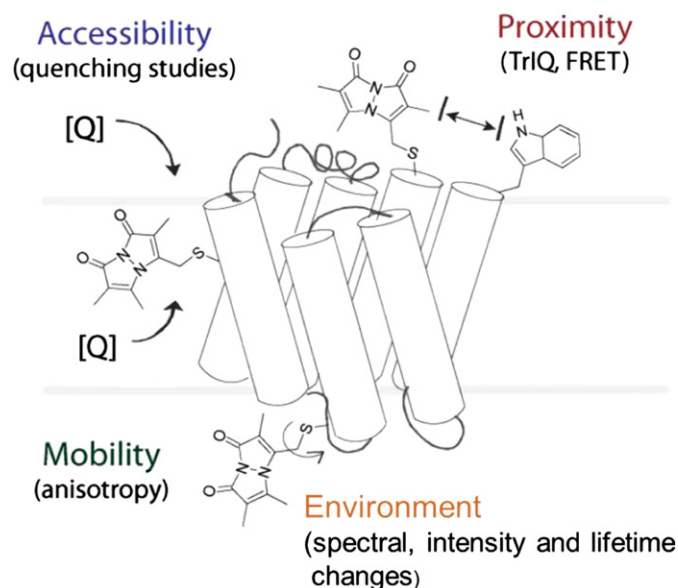
Fig. 9. Cartoon diagram showing the different types of information obtained from SDFL studies of rhodopsin. SDFL studies of rhodopsin are carried out by attaching fluorescent probes to cysteine residues. The fluorescent probe indicated in the figure is a bimane label. Depending on the experiment, the labeled samples are studied to determine the accessibility of the probe, its mobility or its proximity to another fluorophore as well as the changes in its immediate environment.

that do not depend on a 100% labeling stoichiometry, or where concentration is not of concern. A low labeling stoichiometry is even required when working with membranes and performing anisotropy studies to prevent homo-energy transfer (see Section 4.3). However, for testing the functionality of the labeled protein, a labeling stoichiometry close to 100% is mandatory [59].

The labeling stoichiometry can be calculated spectroscopically from the absorbance of rhodopsin (A_{Rho}) and the absorbance of the fluorophore (ΔA_F) at its peak wavelength:

$$\frac{[F]}{[Rho]} = \frac{\Delta A_F}{A_{Rho}} \frac{\varepsilon(Rho)}{\varepsilon(F)} \qquad (12)$$

with ε (Rho) and ε (F) the extinction coefficients of rhodopsin and the fluorophore at the respective wavelengths. Often the absorbance band of the fluorophore overlaps with rhodopsin absorbance. Thus, a difference spectrum between the unlabeled and labeled rhodopsin has to be recorded in order to determine the absorbance of the fluorophore ΔA_F (see for example [26,57,62,70]).

Covalent labeling is usually tested by SDS (sodium dodecyl sulfate) polyacrylamide gel electrophoresis to ensure that the label is attached to the protein. The presence of free, unattached label can also be assessed by comparing the sample before and after TCA (trichloroacetic acid) precipitation and centrifugation.

5.2.1. Examples of accessibility studies on rhodopsin

External fluorescence quencher such as the charged collisional quencher KI (I⁻) can be used to investigate the accessibility of the covalently bound fluorescent probe and its changes upon formation of intermediate states. For example, the accessibility of different parts of the cytoplasmic surface of bovine rhodopsin was studied this way. It was shown that a fluorophore bound to position 316 of the cytoplasmic helix 8 (H8) in rhodopsin (Fig. 10) is highly accessible in the dark state, but the accessibility decreases upon formation of MII [73]. This indicates a change in the conformation of H8 or in its close vicinity, resulting in shielding of the fluorophore [29,73].

Interestingly, a fluorescent probe on the inner face of transmembrane helix 6 (TM6) (Fig. 10) shows almost the exact opposite behavior — lower accessibility for dark-state rhodopsin, and increased collisional quenching for the active MII state [57,91]. Similar behavior is observed

for a probe on TM6 of parapinopsin (a nonvisual rhodopsin that does not hydrolyze the retinal SB linkage) [92].

When carrying out quenching studies of retinal proteins, it is critical to take into account changes in FRET from the fluorophore to the retinal during the measurements. For example, if FRET to the retinal is decreased, the fluorescence lifetime of the attached probe will increase. In such a situation the probe would now have increased time to collide with a quencher molecule, and more apparent quenching might be observed, even if no actual change in physical accessibility of the probe has occurred. To avoid this potential artifact, one converts the Stern–Volmer quenching values (K_{SV}) typically obtained as:

$$\frac{I_o}{I} = 1 + K_{SV} \cdot [Q] \qquad (13)$$

where I_o and I are the intensities of the fluorescence before and after addition of the KI quenching agent (Q), respectively. In a typical Stern–Volmer experiment, the data are usually plotted using the above relationship (where [Q] is the x-axis, and I_o/I is the y-axis, see Fig. 2C and D), and the K_{SV} values are obtained from the slope of the line. To correct for changes in lifetime of the fluorescent probe (caused by changes in FRET from fluorophore to retinal), a modified form of the Stern–Volmer relationship is used to include the measured fluorescence lifetime of the probe:

$$\frac{I_o}{I} = 1 + k_q \cdot \tau_0 \cdot [Q] \qquad (14)$$

with τ_0 the measured fluorescence lifetime, and k_q the bimolecular quenching constant (obtained from the relationship $k_q = K_{SV}/\tau_0$) [57,92].

5.2.2. Examples of proximity studies by FRET and TrIQ

A historic FRET experiment on visual rhodopsin was performed in 1972 by Wu and Stryer [16]. These authors used the binding of various organic dyes to specific reactive native cysteines in visual rhodopsin and their energy transfer to retinal as well as between pairs of dyes to extract information about the general shape of rhodopsin and possible functional relevance.

In a recent example, FRET was combined with FTIR measurements to obtain insight into transmembrane helix–lipid couplings and their impact on a key protonation switch (E134) in the activation of visual rhodopsin
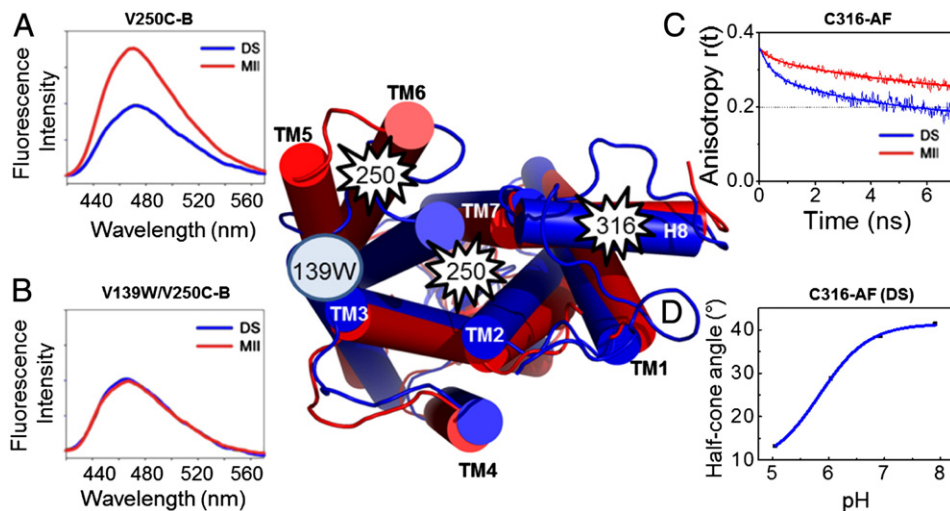
Fig. 10. Structural model of the dark (blue; PDB ID: 1U19) and light-activated (red; PDB ID: 3PXO) state of rhodopsin (center). The positions 250 and 316 to which the fluorescent probes were bound as well as the tryptophan in position 139 are marked. (A) Emission spectra of the bimane probe bound to position 250 in the dark and MII state. (B) Emission spectra of the bimane probe bound to position 250 in the presence of a tryptophan in position 139. The presence of the tryptophan decreases the fluorescence emission in the MII state, indicating a closer interaction between these two positions in MII facilitated by the movement of TM6. (C) Time-resolved anisotropy curves of fluorescein bound to H8 (position 316) in the dark and MII state. (D) The conformational space of H8 in the dark state (expressed as the half cone angle θ [29]) as a function of pH.

[93]. In these experiments, the energy transfer from a tryptophan residue in position 126 of transmembrane helix 3 (TM3) in bovine rhodopsin to dansyl-labeled lipids together with infrared measurements indicated a lipid-mediated coupling mechanism to the protonation state of the conserved E134 in the D(E)RY motif.

Several FRET studies have been performed to investigate rhodopsin–rhodopsin interactions and rhodopsin interactions with other proteins. These include studies of the phototaxis receptor sensory rhodopsin and interactions with its transducer molecule, and structures of the cytoplasmic loops of sensory rhodopsin II and the membrane-proximal cytoplasmic domain of its bound transducer in the dark and in the light-activated state [64]. FRET studies were also used to investigate conformational changes in the phoborhodopsin/transducer complex during the photocycle [63].

Another important application of FRET is the evaluation of binding stoichiometries, and this approach has been used for studying interactions of sensory rhodopsin II with its cognate transducer NpHtrII [60]. Similarly, the self-association of visual rhodopsin in lipid vesicles [61] and COS cells [50], as well as the absence of dimer or oligomer formation for the preparation of monomeric rhodopsin in detergent solution [51] and in nanodiscs [94] have also been studied using FRET. Apart from FRET, fluorescence correlation spectroscopy (FCS) is highly suitable to investigate intermolecular protein binding, as shown for the sensory rhodopsin II/transducer complex [95].

An alternate approach to FRET for protein studies, sometimes called TrIQ (for Trp-Induced Quenching), has also been used for rhodopsin studies [91,92]. Most of the TrIQ studies for protein structural studies employ the fluorophore bimane, although TrIQ also works with other fluorophores of different sizes and spectral properties. The distance over which TrIQ is observed scales with the size of the fluorescent probe [24]. Examples of TrIQ studies on retinal proteins are discussed in Section 6.

5.2.3. Examples of mobility studies

Time-resolved anisotropy experiments allow for the evaluation of diffusional dynamics and conformations, in particular of surface elements of membrane proteins [29]. The fluorescent probe also reflects the steric constraints imposed by the surrounding protein structure. Early anisotropy studies were performed using a fluorescent dye coupled to the C-terminus of bR to evaluate possible secondary structural motifs [96]. Recent studies mainly focus on bR and visual rhodopsin. For example, a switch between two different conformations of the third cytoplasmic loop connecting helix E and F in bR was observed that was triggered by a change in surface potential [26]. Since helix F (helix F in bR corresponds to TM6 in visual rhodopsin) is known to move in the second part of the bR photocycle and in the same time range a transient surface potential change was observed [55], it was proposed that the electrostatically triggered loop conformational change facilitates the movement of helix F [26]. In visual rhodopsin, loop dynamics and conformational changes were shown to correlate with the different photo-intermediates states and the interaction of affiliated proteins involved in signal transduction [26,29,59,70,72,73,88,97]. Fluorescence pump–probe experiments using multi-dimensional TCSPC allow to investigate the time-course of protein dynamics and conformational changes following light-activation of rhodopsins [59,71]. Another line of mobility studies is concerned with the investigation of couplings between lipid dynamics and retinal protein activation [98,99]. A more in-depth discussion of these studies will be provided in Section 6.

5.2.4. Examples of environmental changes

The local polarity experienced by a fluorescent probe usually affects its spectral properties, and this information can be used to gain insights about the apparent polarity and solvent accessibility around the site of label attachment. For example, the fluorescence excitation and emission spectra of the probe bimane are blue-shifted with lower solvent polarity [100]. Detailed studies of T4 Lysozyme have established that the bimane emission maximum reliably reflects the relative polarity (and by

inference solvent accessibility) of the fluorescent probe where it is attached to the protein [100,101]. Thus, as discussed later in Section 6, shifts in bimane fluorescence properties can be used to monitor conformational changes in rhodopsin and to monitor protein–protein interactions. Besides bimane, other dyes (Alexa594, Lucifer Yellow, fluorescein) are affected as well by the conformational changes occurring upon light-activation of rhodopsin [58,59,70,72].

6. From molecular to cellular insight in visual rhodopsin function

6.1. Conformational plasticity of rhodopsin

Essentially, the entire cytoplasmic face of visual rhodopsin has been studied by Khorana and colleagues using site-directed labeling methods, mostly EPR spectroscopy and cysteine reactivity measurements [52,57,102], although F19 NMR [102] and fluorescence (SDFL) studies have also been used (see below).

In all of these studies, the largest changes accompanying light activation were observed for probes placed on or near TM6 (see Fig. 10). The data led to the hypothesis that some kind of tilt and/or rotation of TM6 occurs upon rhodopsin activation [57,102–104], although changes for fluorescent probes attached at H8 have also suggested movements in that region as well [58,59,70,72,73,97]. These conformational changes are important for molecular recognition and activation of the G-protein transducin that initiates the enzymatic cascade of phototransduction and for the binding of arrestin that is involved in the deactivation process of rhodopsin.

6.1.1. TM6 movements in rhodopsin upon light activation

The necessity of TM6 movement to enable coupling with G-proteins was suggested from experiments that found that linking TM6 together with TM3 through disulfides [103,104] or a zinc binding site [105] severely impaired G-protein activation by rhodopsin. In contrast, disulfide cross-links at other sites in rhodopsin have no effect on its ability to activate G-protein [103,106]. Interestingly, TM6 movement may be a universal feature of retinal proteins, as it is observed during light activation of many other light-sensitive retinal proteins, including bacteriorhodopsin [107–110], and sensory rhodopsin [111–116].

Following this, fluorescence studies have suggested that the magnitude of TM6 movement in rhodopsins, as well as other GPCRs, correlates with their ability to activate G-proteins. Early studies established that TM6 movement in rhodopsin could be detected using the TrIQ approach by monitoring the quenching of a bimane fluorophore on TM6 (Fig. 10A and B) by tryptophan residues introduced on TM3 [52]. Subsequent TrIQ studies used this approach to compare transmembrane helix movements in rhodopsin and parapinopsin and found that TM6 movements were less in parapinopsin, providing a possible explanation for why parapinopsin is ~20× less effective at activating G-proteins than rhodopsin [92]. Similarly, Kobilka and colleagues used TrIQ to determine that TM6 movement in the beta-2-adrenergic receptor is only observed upon binding of receptor activating ligands (agonists), whereas no movement was seen with antagonists [117]. Fluorescence studies of the cannabinoid receptor CB1 also indicate ligand-induced conformational changes at TM6, which are blocked upon binding of the inverse agonist ORG2716 [118]. Together, these studies suggest TM6 movements may be a universal requirement not only in opsins, but also in other GPCRs.

The observed large conformational changes of rhodopsin upon light-activation and formation of the active MII intermediate are tightly coupled to the interactions of the protein with the membrane lipids. A series of time-resolved fluorescence anisotropy studies revealed a direct correlation between lipid acyl chain ordering and MII formation [98,99].

6.1.2. TM6 movement enables binding of the G-protein Gα C-terminus to a "hydrophobic patch" on rhodopsin

The question of why TM6 movement occurs in rhodopsin was addressed using a combination of SDFL methods, including TrIQ. The

hypothesis was that TM6 movement exposes a binding site for the transducin Gα subunit (GTα) C-terminal tail (GTα C-term). The GTα C-term was known to be required for rhodopsin–transducin interaction [119], and peptide analogs of this region bind rhodopsin with high affinity [120] and become structured in the process [121,122].

The fluorescence studies found that the TM6 movement in rhodopsin exposes a necessary hydrophobic binding site for the GTα C-term. Fluorescence quenching studies showed that a bimane probe on the inner face of TM6 (at site V250, Fig. 10) was shielded from quencher molecules upon binding of peptides corresponding to the GTα C-term. This result is consistent with previous studies suggesting a role for this region of rhodopsin for GTα C-term interaction [123,124]. The rhodopsin–GTα C-term interactions were further studied by TrIQ. Rhodopsin mutants with bimane labels placed at different sites on the cytoplasmic face were incubated with a GTα C-term peptide containing a tryptophan residue, and sites of contact were identified by the decrease of bimane fluorescence upon peptide binding (i.e. increase in TrIQ). A subset of these sites was further studied by introducing mutations on the inner face of transmembrane helix 5 (TM5) that were known to impair transducin activation [52]. These TrIQ studies revealed a high affinity interaction between hydrophobic residues in rhodopsin (L226, T229 and V230) and the GTα C-term, with each of these residues contributing ~3 kcal/mol binding energy. Based on these results, it was proposed that TM6 movement occurs in rhodopsin during light activation to expose the "hydrophobic patch" in rhodopsin (made up of residues L226, T229 and V230), that then directly interacts with hydrophobic residues in the GTα C-terminal tail of transducin [91]. Subsequent high-resolution crystal structures of "active opsin" bound to a similar GTα C-term peptide are in excellent agreement with this hypothesis [125], showing specific hydrophobic residues in the "hydrophobic patch" on rhodopsin making extensive interactions with hydrophobic residues on the GTα C-term.

6.1.3. Fluorescently labeled GTα C-term as an affinity label for MII in single molecule studies

Since peptide analogs of the GTα C-term bind to MII with high affinity, a single molecule method was developed that employs a fluorescently labeled GTα C-term to tag single rhodopsin molecules in their active MII state [74]. Single molecule studies can give direct information about how individual molecules move and interact in the cellular context. Thus, the approach was combined with total internal reflection fluorescence (TIRF) microscopy, where an evanescent field excites only fluorophores in close distance to a glass surface, thereby being specific to the proteins interacting with the rhodopsin disk membranes deposited on the glass slide surface. Three experiments were governed that way: 1) binding kinetics of transducin derived peptides or transducin can be measured at the single molecule level [74,97]. Briefly, after a short flash of light to activate rhodopsin, the interactions are monitored by time-lapse microscopy. The number of spots in the image at a given time point, indicative of fluorescently labeled GTα C-term bound to the light-activated rhodopsins in the disk membrane (designated pGTα-F in Fig. 11), was counted and plotted as a function of time after rhodopsin activation. Thus, the classical biophysical approach in which the binding of transducin or transducin peptides to light-activated rhodopsin was measured by kinetic light-scattering experiments [126] is now extended to the single molecule level. 2) The lateral diffusion of activated rhodopsin was followed using single particle tracking [74,97]. Heterogeneous diffusion behavior and confined motion of light-activated rhodopsins in disk membranes were found, compatible with disk membrane inhomogeneity and a semi-ordered packing of rhodopsin at a time scale which corresponds to the millisecond activation time scale of rhodopsin. 3) Using the inherent high spatial information density in single particle tracking experiments, so called visits maps were reconstructed that allow for an identification of hotspots or places of affine binding at the rhodopsin membrane with spatial resolution below the diffraction limit [29,97].
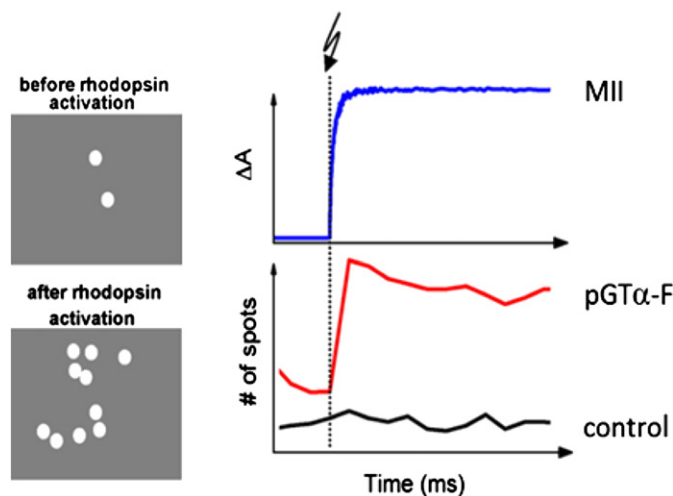

Fig. 11. Single molecule TIRF experiments of rhodopsin disk membranes. Kinetic single molecule binding assay for signaling molecules, here with pGTα-F (red trace), a fluorescently labeled transducin derived peptide, which stabilizes MII [74]. For comparison, the time trace of MII formation (ΔA at 380 nm) is shown. The schematic shows individual fluorescently labeled transducin molecules (white dots) interacting with rhodopsin containing disk membranes.

6.1.4. Helix 8 movements in rhodopsin upon light activation

Since the first x-ray crystal structure of rhodopsin [127] resolved the fourth cytoplasmic loop between TM7 and the two palmitoylated cysteines 322 and 323 as a helical structure lying parallel to the membrane surface (Figs. 6 and 10), it was anticipated that this helix (H8) plays an important role in the GPCR signaling process due to its amphipathic properties. Located at the start of the C-terminal tail of class A GPCRs, it might serve as a transmitter of signaling states or be involved in regulating the structure of the C-terminus. Coupling of H8 to the ligand binding pocket is mediated by the interhelical network (including transmembrane helix 1 (TM1), 2 (TM2), and TM7) that connects D83 (TM2) to the conserved NPxxY motif in TM7 preceding H8.

To analyze the structural dynamics of H8 in the different states of the functional cycle of rhodopsin, time-resolved fluorescence spectroscopy [71] combined with SDFL of C316 in H8 was employed [26,29,59,70, 72,73,88,97]. Residue 316 resides on the solvent exposed surface of H8 (Figs. 6 and 10). The change in fluorescence intensity of certain fluorescence probes attached to H8 via C316 mirrors the equilibrium between the metarhodopsin-I (MI) and MII state [58,70,72]. These results indicate environmental changes at the cytoplasmic surface of rhodopsin in the vicinity of H8, which are connected to the transition into the active receptor state. A direct correlation of H8 conformational changes with the active receptor state MII was shown by FTIR/fluorescence cross-correlation spectroscopy [72]. These studies revealed a high correlation of the surface alterations around H8 with H-bonding to D83 proximal of the retinal SB and with MII specific 1643 cm^{-1} IR absorption changes, indicative of a partial loss of secondary structure of H8 upon MII formation [72]. The correlations were maintained upon binding of a GTα C-term peptide [72]. However, since these conformational changes seem to differ from those observed in the presence of transducin in another study [58], this suggests that the conformation of the cytoplasmic surface around H8 is different in the rhodopsin–transducin complex.

To provide a more in-depth characterization, the internal dynamics of H8 as a function of the ligand-binding pocket (i.e. in the absence and presence of retinal) was systematically analyzed in the dark state, after light activation in the MII state, as well as after phosphorylation [59,70,97]. In the dark state of rhodopsin the restriction of H8-diffusional motion by the constituents of the protein surface is dependent on pH [26], as illustrated in Fig. 10D. This pH dependence coincides with the pH-dependence of the MI/MII equilibrium suggesting an

alkaline "unlock" of H8 in the dark state possibly preventing activation of rhodopsin [26]. High mobility of H8 in the dark state was also observed to correspond with a shift of the MI/MII equilibrium toward the inactive precursor state MI [29,70].

Upon formation of the active receptor state MII, the steric restriction and rotational correlation time of H8 diffusional motion increases (Fig. 10C), compatible with additional contacts mediated by the C-terminal tail as indicated from the FTIR experiments [72]. These results suggested that an increase in size, due to additional contacts with the long C-terminal tail, as well as a shape change based on partial loss of H8 secondary structure are responsible for the slower diffusion of H8 in MII. This conclusion is also supported by the finding of a reduced accessibility of H8 from the solvent in MII [73], when probed with a charged collisional quencher (I⁻). In summary, these studies indicate that H8 in the active MII state is shielded and kept in position by additional contacts from the long C-terminal tail, which folds back toward H8 [29].

6.2. Protein–protein interactions involved in rhodopsin deactivation

Interactions of rhodopsin with arrestin have been monitored in a number of ways using fluorescence approaches. For example, arrestin binding has been detected using probes on rhodopsin [58,59]. The process of deactivation starts when MII is phosphorylated at specific serine and/or threonine residues at its C-terminal tail by rhodopsin kinase, followed by high-affinity binding of visual arrestin to phosphorylated light-activated rhodopsin (Rho*-P) [128–130]. Investigations of the H8 behavior in Rho*-P, using the anisotropy approaches described above, showed only minor changes in H8 diffusional properties compared to the dark state. Both, the slower rotational diffusion of H8 and the increased steric restriction of diffusion seen for active MII are nearly absent in Rho*-P [29,59,97]. These results suggest that phosphorylation of the C-terminal tail probably disrupts MII-specific contacts between H8 and the C-terminus, which subsequently leads to a decoupling between the ligand binding pocket and H8 and to a destabilization of the active cytoplasmic MII conformation. This interpretation agrees with experimental data and simulations [131,132], showing partial rhodopsin (MII) deactivation upon rhodopsin phosphorylation. Thus, phosphorylation of the long C-terminal tail serves two functions: 1) enabling high-affinity arrestin binding, and 2) decoupling of H8 from the intramolecular interactions with the ligand binding pocket and promoting H8 accessibility from the solvent. Decoupling of H8 dynamics might facilitate arrestin binding in a sense that it serves as a transmitter of the receptor signaling state to interacting arrestin molecules in an early encounter state.

Further studies using time-resolved fluorescence spectroscopy combined with SDFL of C316 showed that conformational dynamics of H8 controls the binding of arrestin [59]. At least two sequential conformational changes of arrestin occur upon interaction with Rho*-P, thus providing a kinetic proof for the suggested multistep nature of arrestin binding. The structural dynamics of the amphipathic H8, connecting TM7 and the phosphorylated C-terminal tail, depends on the arrestin interaction state. A high mobility of H8 is required in the low-affinity (pre-binding), but not in the high-affinity binding state. A close steric interaction of H8 with arrestin is mandatory for the transition from pre-binding to high-affinity binding; i.e., for arrestin activation. These findings imply a regulatory role for H8 in activation of visual arrestin [59].

Other studies have placed fluorescent probes on arrestin and monitored the fluorescence changes that occur when arrestin binds to Rho*-P. These investigations have been carried out both in native rod outer segments (ROS) membranes [59,81,133], as well as with Rho*-P in detergent [134]. A bimane probe in the so-called "finger loop" of arrestin at site 72 (I72B) proved especially informative, at it shows a dramatic increase and blue shift in emission upon binding Rho*-P, indicating that upon binding the environment around the bimane for I72B becomes more hydrophobic, either because the probe becomes buried in a protein–protein or in a protein–lipid interface. The majority of

changes detected by I72B are reverted when retinal and arrestin are released from Rho*-P. However, it was noticed that a small subset of the changed fluorescence signal did not revert to its original value, suggesting that some of the arrestin had remained bound to the phosphorylated rhodopsin [81]. This phenomenon was explored further and ultimately led to the development of a fluorescence assay for monitoring not only arrestin binding, but also arrestin release. Use of this assay led to several new discoveries, including the fact that acidic lipids are required for arrestin binding to Rho*-P in detergent [134], and that arrestin can bind to MIII rhodopsin and influence its absorption spectrum [134], as well as influence other photoproducts [134].

The relative stoichiometries of arrestin interactions with visual rhodopsin, as well as rhodopsin with other affiliate proteins like transducin and rhodopsin kinase, have been the source of intense interest. Visual rhodopsin, like other GPCRs, has been proposed to self-associate into dimers and higher order species, a concept initially put forward by Palczewski and colleagues [135] based on atomic force microscopy studies. Subsequent fluorescent studies also found clear evidence for self-association of visual rhodopsin, including work using purified, labeled rhodopsin reconstituted into lipid vesicles [61], and studies of GFP-tagged opsin in COS cell membranes [50]. The question of stoichiometry became even more clouded given subsequent work that found only one rhodopsin is needed to interact with any of its affiliate binding partners, arrestin [94,136], transducin [137–139] or rhodopsin kinase [136]. Thus, over the years a number of conflicting models have been proposed for the stoichiometry between interacting affiliate proteins and rhodopsin, ranging from 1:1 to 2:1 or higher [140,141]. However, in the case of arrestin interactions with rhodopsin, the options suggested in the conflicting models described above may not be mutually exclusive. Based on the unusual behavior in the fluorescence assays described in the preceding paragraph, in which fluorescently-labeled I72B arrestin monitored binding to rhodopsin and trapping of some of the retinal, a tentative hypothesis was formulated that arrestin might, under some conditions (and for unknown reasons), be able to bind two rhodopsin molecules at the same time, thus trapping the retinal in one of them [Sommer and Farrens, unpublished data]. This idea was later expanded on in a series of elegant studies finding evidence that arrestin can bind to either monomeric or multimeric rhodopsin in ROS membranes, depending on the amount of photoactivated rhodopsin present [142]. Interestingly, it appears that interactions of different loops in arrestin are able to affect the bound retinal status of rhodopsin [143].

7. Concluding remarks and future directions

Fluorescence instrumentation and methodologies continue to develop at a rapid pace. However, the fundamental processes an experimentalist exploits when he or she excites a fluorophore and monitors the light being emitted are unchanged. In this chapter, we briefly reviewed these processes, and discussed why, how and what information can be gleaned about rhodopsins using fluorescence approaches. We also covered some of the unique challenges facing an experimentalist carrying out fluorescence studies on rhodopsins, and showed how some of these issues can be dealt with, and even be exploited at times to gain understanding of the dynamic changes the rhodopsin proteins undergo, both during and after the photo-activation process.

What does the future hold for fluorescence studies of rhodopsin proteins? Certainly the fluorescence methods, analysis, and caveats we have covered in this chapter also pertain to the exciting new "designer" retinal proteins that are increasingly being used both as bio-sensors and as light-activated signaling devices. However, the future of fluorescence studies on traditional rhodopsins is also "bright", especially as it continues to combine ever-improving spectroscopic techniques such as single molecule methods [74,97] and TrIQ [91,102] with advances in molecular and biochemical methods (such as nanodiscs [138]).

One example of the convergence of these emerging technologies involves the study of rhodopsin using a combination of nanodisc

technologies with single molecule fluorescence measurements. Nanodiscs, also called nanoscale apolipoprotein-bound bilayers (NABBs), are small patches of membrane bilayer surrounded by a membrane scaffolding protein (MSP), a derivative of apolipoprotein A1. These "lipid sandwiches" have a number of unique properties. They are soluble, only approximately 10 nm in diameter, and can be used to incorporate rhodopsins at defined stoichiometries, i.e. one or two per nanodisc. Rhodopsin-nanodisc preparations show very little light scattering, thus their optical properties are ideal and facilitate fluorescence studies. Visual rhodopsin preparations in nanodiscs have been shown to produce photointermediates that are very similar to those in native membrane [94], and the active receptor can vigorously couple with the G-protein transducin [137–139], arrestin [94,136], and rhodopsin kinase [136]. The ability of nanodiscs to encapsulate defined lipids makes it possible to measure the effect of lipid compositions on rhodopsin and its interaction with other proteins [94,144]. Moreover, since incorporation of rhodopsin into nanodiscs is relatively efficient, mutant rhodopsin proteins can be investigated this way [145]. Furthermore, it is possible to study single rhodopsin-containing nanodiscs by attaching them to a glass slide and then employing total internal reflection fluorescence (TIRF) microscopy. TIRF exploits an evanescent field that only covers a short distance above the glass surface to selectively excite fluorophores within this field, and can be used to study many aspects of fluorescence, such as changes in intensity and FRET. Since the nanodiscs attached to the slide cannot drift away, it is possible to measure the properties of a single nanodisc over time.

One exciting prospect to use TIRF is to precisely study the interaction of rhodopsin in nanodiscs with its interacting partner proteins. For example, by repeatedly measuring individual interactions of rhodopsin with a protein like arrestin or transducin, it may be possible to better define kinetic and thermodynamic parameters that more closely reflect the situation *in vivo*, wherein the proteins are interacting at a surface, not in a three dimensional solution containing detergents. Such approaches will also require new methods for assembling and purifying the membrane proteins, as well as labeling them with new and novel fluorophores. Examples of advances in these areas have recently been reviewed [66,146,147].

Acknowledgements

References

[1] D. Oesterhelt, W. Stoeckenius, Functions of a new photoreceptor membrane, Proc. Natl. Acad. Sci. U. S. A. 70 (1973) 2853–2857.
[2] J.P. Klare, I. Chizhov, M. Engelhard, Microbial rhodopsins: scaffolds for ion pumps, channels, and sensors, Results Probl. Cell Differ. 45 (2008) 73–122.
[3] U. Alexiev, R. Mollaaghababa, P. Scherrer, H.G. Khorana, M.P. Heyn, Rapid long-range proton diffusion along the surface of the purple membrane and delayed proton transfer into the bulk, Proc. Natl. Acad. Sci. U. S. A. 92 (1995) 372–376.
[4] J.K. Lanyi, Halorhodopsin: a light-driven chloride ion pump, Annu. Rev. Biophys. Biophys. Chem. 15 (1986) 11–28.
[5] J.P. Klare, V.I. Gordeliy, J. Labahn, G. Buldt, H.J. Steinhoff, M. Engelhard, The archaeal sensory rhodopsin II/transducer complex: a model for transmembrane signal transfer, FEBS Lett. 564 (2004) 219–224.
[6] J.L Spudich, The multitalented microbial sensory rhodopsins, Trends Microbiol. 14 (2006) 480–487.
[7] P. Hegemann, Algal sensory photoreceptors, Annu. Rev. Plant Biol. 59 (2008) 167–189.
[8] O.A. Sineshchekov, E.G. Govorunova, J.L. Spudich, Photosensory functions of channelrhodopsins in native algal cells, Photochem. Photobiol. 85 (2009) 556–563.
[9] G. Nagel, D. Ollig, M. Fuhrmann, S. Kateriya, A.M. Musti, E. Bamberg, P. Hegemann, Channelrhodopsin-1: a light-gated proton channel in green algae, Science 296 (2002) 2395–2398.
[10] V.Y. Arshavsky, M.E. Burns, Photoreceptor signaling: supporting vision across a wide range of light intensities, J. Biol. Chem. 287 (2011) 1620–1626.
[11] D.A. Baylor, T.D. Lamb, K.W. Yau, Responses of retinal rods to single photons, J. Physiol. 288 (1979) 613–634.
[12] T. Yoshizawa, G. Wald, Pre-lumirhodopsin and the bleaching of visual pigments, Nature 197 (1963) 1279–1286.
[13] G. Wald, The molecular basis of visual excitation, Nature 219 (1968) 800–807.
[14] T.W. Cronin, T.H. Goldsmith, Fluorescence of crayfish metarhodopsin studied in single rhabdoms, Biophys. J. 35 (1981) 653–664.
[15] A.V. Guzzo, G.L. Pool, Fluorescence spectra of the intermediates of rhodopsin bleaching, Photochem. Photobiol. 9 (1969) 565–570.
[16] C.W. Wu, L. Stryer, Proximity relationships in rhodopsin, Proc. Natl. Acad. Sci. U. S. A. 69 (1972) 1104–1108.
[17] J.W. Borst, A.J.W.G. Visser, Fluorescence lifetime imaging microscopy in life sciences, Meas. Sci. Technol. 21 (2010).
[18] J.R. Lakowicz, Principles of Fluorescence Spectroscopy, Springer, 2006.
[19] M. Sauer, J. Hofkens, J. Enderlein, Handbook of Fluorescence Spectroscopy Imaging, Wiley-VCH, 2011.
[20] M.R. Eftink, C.A. Ghiron, Fluorescence quenching studies with proteins, Anal. Biochem. 114 (1981) 199–227.
[21] D.L. Dexter, A Theory of Sensitized Luminescence in Solids, J. Chem. Phys. 21 (1953) 836–850.
[22] A.P. de Silva, T.S. Moody, G.D. Wright, Fluorescent PET (Photoinduced Electron Transfer) sensors as potent analytical tools, Analyst 134 (2009) 2385–2393.
[23] S. Doose, H. Neuweiler, M. Sauer, Fluorescence quenching by photoinduced electron transfer: a reporter for conformational dynamics of macromolecules, ChemPhysChem 10 (2009) 1389–1398.
[24] S.E. Mansoor, M.A. Dewitt, D.L. Farrens, Distance mapping in proteins using fluorescence spectroscopy: the tryptophan-induced quenching (TrIQ) method, Biochemistry 49 (2010) 9722–9731.
[25] T. Förster, Zwischenmolekulare Energiewanderung und Fluoreszenz, Ann. Phys. 437 (1948) 55–75.
[26] U. Alexiev, I. Rimke, T. Pohlmann, Elucidation of the nature of the conformational changes of the EF-interhelical loop in bacteriorhodopsin and of the helix VIII on the cytoplasmic surface of bovine rhodopsin: a time-resolved fluorescence depolarization study, J. Mol. Biol. 328 (2003) 705–719.
[27] K. Kinosita, S. Kawato, A. Ikegami, A theory of fluorescence polarization decay in membranes, Biophys. J. 20 (1977) 289–305.
[28] G.F. Schroder, U. Alexiev, H. Grubmuller, Simulation of fluorescence anisotropy experiments: probing protein dynamics, Biophys. J. 89 (2005) 3757–3770.
[29] T.-Y. Kim, T. Schlieter, S. Haase, U. Alexiev, Activation and molecular recognition of the GPCR rhodopsin — insights from time-resolved fluorescence depolarisation and single molecule experiments, Eur. J. Cell Biol. 91 (2012) 300–310.
[30] H. Kandori, Y. Furutani, S. Nishimura, Y. Shichida, H. Chosrowjan, Y. Shibata, N. Mataga, Excited-state dynamics of rhodopsin probed by femtosecond fluorescence spectroscopy, Chem. Phys. Lett. 334 (2001) 271–276.
[31] T. Kouyama, K. Kinosita, A. Ikegami, Excited-state dynamics of bacteriorhodopsin, Biophys. J. 47 (1985) 43–54.
[32] A.G. Doukas, M.R. Junnarkar, R.R. Alfano, R.H. Callender, T. Kakitani, B. Honig, Fluorescence quantum yield of visual pigments — evidence for subpicosecond isomerization rates, Proc. Natl. Acad. Sci. U. S. A. 81 (1984) 4790–4794.
[33] M.O. Lenz, R. Huber, B. Schmidt, P. Gilch, R. Kalmbach, M. Engelhard, J. Wachtveitl, First steps of retinal photoisomerization in proteorhodopsin, Biophys. J. 91 (2006) 255–262.
[34] J.M. Kralj, D.R. Hochbaum, A.D. Douglass, A.E. Cohen, Electrical spiking in *Escherichia coli* probed with a fluorescent voltage-indicating protein, Science 333 (2011) 345–348.
[35] J.M. Kralj, A.D. Douglass, D.R. Hochbaum, D. Maclaurin, A.E. Cohen, Optical recording of action potentials in mammalian neurons using a microbial rhodopsin, Nat. Methods 9 (2012) 90–95.
[36] R. Huber, T. Kohler, M.O. Lenz, E. Bamberg, R. Kalmbach, M. Engelhard, J. Wachtveitl, pH-dependent photoisomerization of retinal in proteorhodopsin, Biochemistry 44 (2005) 1800–1806.
[37] M.O. Lenz, A.C. Woerner, C. Glaubitz, J. Wachtveitl, Photoisomerization in proteorhodopsin mutant D97N, Photochem. Photobiol. 83 (2007) 226–231.
[38] S.P. Balashov, F.F. Litvin, V.A. Sineshchekov, Photochemical processes of light energy transformation in bacteriorhodopsin, Physicochemical Biology Reviews, Gordon & Breach Publishing Group, 1988. 1–61.
[39] L. Song, M.A. Elsayed, J.K. Lanyi, Protein catalysis of the retinal subpicosecond photoisomerization in the primary process of bacteriorhodopsin photosynthesis, Science 261 (1993) 891–894.
[40] D. Maclaurin, V. Venkatachalam, H. Lee, A.E. Cohen, Mechanism of voltage-sensitive fluorescence in a microbial rhodopsin, Proc. Natl. Acad. Sci. U. S. A. 110 (2013) 5939–5944.
[41] E.N. Laricheva, S. Gozem, S. Rinaldi, F. Melaccio, A. Valentini, M. Olivucci, Origin of fluorescence in 11-cis locked bovine rhodopsin, J. Chem. Theory Comput. 8 (2012) 2559–2563.
[42] H. Kandori, S. Matuoka, Y. Shichida, T. Yoshizawa, M. Ito, K. Tsukida, V. Baloghnair, K. Nakanishi, Mechanism of isomerization of rhodopsin studied by use of 11-cis-locked rhodopsin analogs excited with a picosecond laser-pulse, Biochemistry 28 (1989) 6460–6467.
[43] J. Peters, R. Peters, W. Stoeckenius, A photosensitive product of sodium borohydride reduction of bacteriorhodopsin, FEBS Lett. 61 (1976) 128–134.
[44] D. Bownds, G. Wald, Reaction of rhodopsin chromophore with sodium borohydride, Nature 205 (1965) 254–257.
[45] T.G. Ebrey, Energy transfer in rhodopsin, N-retinyl-opsin, and rod outer segments, Proc. Natl. Acad. Sci. U. S. A. 68 (1971) 713–716.
[46] D. Rhinow, M. Imhof, I. Chizhik, R.P. Baumann, N. Hampp, Structural changes in bacteriorhodopsin caused by two-photon-induced photobleaching, J. Phys. Chem. B 116 (2012) 7455–7462.

[47] S.C. Hovan, S. Howell, P.S. Park, Forster resonance energy transfer as a tool to study photoreceptor biology, J. Biomed. Opt. 15 (2010) 067001.

[48] C. Schmitt, C. Schultheis, S.J. Husson, J.F. Liewald, A. Gottschalk, Specific expression of channelrhodopsin-2 in single neurons of *Caenorhabditis elegans*, PLoS One 7 (2012) e43164.

[49] B.A. Price, I.M. Sandoval, F. Chan, D.L. Simons, S.M. Wu, T.G. Wensel, J.H. Wilson, Mislocalization and degradation of human P23H-rhodopsin-GFP in a knockin mouse model of retinitis pigmentosa, Invest. Ophthalmol. Vis. Sci. 52 (2011) 9728–9736.

[50] P. Kota, P.J. Reeves, U.L. Rajbhandary, H.G. Khorana, Opsin is present as dimers in COS1 cells: identification of amino acids at the dimeric interface, Proc. Natl. Acad. Sci. U. S. A. 103 (2006) 3054–3059.

[51] O.P. Ernst, V. Gramse, M. Kolbe, K.P. Hofmann, M. Heck, Monomeric G protein-coupled receptor rhodopsin in solution activates its G protein transducin at the diffusion limit, Proc. Natl. Acad. Sci. U. S. A. 104 (2007) 10859–10864.

[52] D.L. Farrens, What site-directed labeling studies tell us about the mechanism of rhodopsin activation and G-protein binding, Photochem. Photobiol. Sci. 9 (2010) 1466–1474.

[53] P. Scherrer, U. Alexiev, T. Marti, H.G. Khorana, M.P. Heyn, Covalently bound pH-indicator dyes at selected extracellular or cytoplasmic sites in bacteriorhodopsin. 1. Proton migration along the surface of bacteriorhodopsin micelles and its delayed transfer from surface to bulk, Biochemistry 33 (1994) 13684–13692.

[54] U. Alexiev, T. Marti, M.P. Heyn, H.G. Khorana, P. Scherrer, Surface charge of bacteriorhodopsin detected with covalently bound pH indicators at selected extracellular and cytoplasmic sites, Biochemistry 33 (1994) 298–306.

[55] U. Alexiev, P. Scherrer, T. Marti, H.G. Khorana, M.P. Heyn, Time-resolved surface charge change on the cytoplasmic side of bacteriorhodopsin, FEBS Lett. 373 (1995) 81–84.

[56] H. Borochov-Neori, M. Montal, Rhodopsin-G-protein interactions monitored by resonance energy transfer, Biochemistry 28 (1989) 1711–1718.

[57] T.D. Dunham, D.L. Farrens, Conformational changes in rhodopsin. Movement of helix f detected by site-specific chemical labeling and fluorescence spectroscopy, J. Biol. Chem. 274 (1999) 1683–1690.

[58] Y. Imamoto, M. Kataoka, F. Tokunaga, K. Palczewski, Light-induced conformational changes of rhodopsin probed by fluorescent alexa594 immobilized on the cytoplasmic surface, Biochemistry 39 (2000) 15225–15233.

[59] K. Kirchberg, T.-Y. Kim, M. Möller, D. Skegro, G.D. Raju, J. Granzin, G. Büldt, R. Schlesinger, U. Alexiev, Conformational dynamics of helix 8 in the GPCR rhodopsin controls arrestin activation in the desensitization process, Proc. Natl. Acad. Sci. U. S. A. 108 (2011) 18690–18695.

[60] J. Kriegsmann, M. Brehs, J.P. Klare, M. Engelhard, J. Fitter, Sensory rhodopsin II/transducer complex formation in detergent and in lipid bilayers studied with FRET, Biochim. Biophys. Acta 1788 (2009) 522–531.

[61] S.E. Mansoor, K. Palczewski, D.L. Farrens, Rhodopsin self-associates in asolectin liposomes, Proc. Natl. Acad. Sci. U. S. A. 103 (2006) 3060–3065.

[62] M. Moller, U. Alexiev, Surface charge changes upon formation of the signaling state in visual rhodopsin, Photochem. Photobiol. 85 (2009) 501–508.

[63] Y. Taniguchi, T. Ikehara, N. Kamo, H. Yamasaki, Y. Toyoshima, Dynamics of light-induced conformational changes of the phoborhodopsin/transducer complex formed in the n-dodecyl beta-D-maltoside micelle, Biochemistry 46 (2007) 5349–5357.

[64] C.S. Yang, O. Sineshchekov, E.N. Spudich, J.L. Spudich, The cytoplasmic membrane-proximal domain of the HtrII transducer interacts with the E–F loop of photoactivated *Natronomonas pharaonis* sensory rhodopsin II, J. Biol. Chem. 279 (2004) 42970–42976.

[65] J. Heberle, N.A. Dencher, Surface-bound optical probes monitor protein translocation and surface potential changes during the bacteriorhodopsin photocycle, Proc. Natl. Acad. Sci. U. S. A. 89 (1992) 5996–6000.

[66] K.A. Daggett, T.P. Sakmar, Site-specific in vitro and in vivo incorporation of molecular probes to study G-protein-coupled receptors, Curr. Opin. Chem. Biol. 15 (2011) 392–398.

[67] S. Ye, C. Kohrer, T. Huber, M. Kazmi, P. Sachdev, E.C. Yan, A. Bhagat, U.L. RajBhandary, T.P. Sakmar, Site-specific incorporation of keto amino acids into functional G protein-coupled receptors using unnatural amino acid mutagenesis, J. Biol. Chem. 283 (2008) 1525–1533.

[68] H. Bayraktar, A.P. Fields, J.M. Kralj, J.L. Spudich, K.J. Rothschild, A.E. Cohen, Ultrasensitive measurements of microbial rhodopsin photocycles using photochromic FRET, Photochem. Photobiol. 88 (2012) 90–97.

[69] D. Hoersch, H. Otto, I. Wallat, M.P. Heyn, Monitoring the conformational changes of photoactivated rhodopsin from microseconds to seconds by transient fluorescence spectroscopy, Biochemistry 47 (2008) 11518–11527.

[70] T.Y. Kim, M. Moeller, K. Winkler, K. Kirchberg, U. Alexiev, Dissection of environmental changes at the cytoplasmic surface of light-activated bacteriorhodopsin and visual rhodopsin: sequence of spectrally silent steps, Photochem. Photobiol. 85 (2009) 570–577.

[71] T.Y. Kim, K. Winkler, U. Alexiev, Picosecond multidimensional fluorescence spectroscopy: a tool to measure real-time protein dynamics during function, Photochem. Photobiol. 83 (2007) 378–384.

[72] N. Lehmann, U. Alexiev, K. Fahmy, Linkage between the intramembrane H-bond network around aspartic acid 83 and the cytosolic environment of helix 8 in photoactivated rhodopsin, J. Mol. Biol. 366 (2007) 1129–1141.

[73] T. Mielke, U. Alexiev, M. Glasel, H. Otto, M.P. Heyn, Light-induced changes in the structure and accessibility of the cytoplasmic loops of rhodopsin in the activated MII state, Biochemistry 41 (2002) 7875–7884.

[74] T.Y. Kim, H. Uji-i, M. Moller, B. Muls, J. Hofkens, U. Alexiev, Monitoring the interaction of a single G-protein key binding site with rhodopsin disk membranes upon light activation, Biochemistry 48 (2009) 3801–3803.

[75] R. Henderson, J.M. Baldwin, T.A. Ceska, F. Zemlin, E. Beckmann, K.H. Downing, Model for the structure of bacteriorhodopsin based on high-resolution electron cryo-microscopy, J. Mol. Biol. 213 (1990) 899–929.

[76] S. Filipek, Organization of rhodopsin molecules in native membranes of rod cells—an old theoretical model compared to new experimental data, J. Mol. Model. 11 (2005) 385–391.

[77] D.L. Farrens, H.G. Khorana, Structure and function in rhodopsin. Measurement of the rate of metarhodopsin II decay by fluorescence spectroscopy, J. Biol. Chem. 270 (1995) 5073–5076.

[78] A. Kropf, Intramolecular energy transfer in rhodopsin, Vision Res. 7 (1967) 811–818.

[79] M. Heck, S.A. Schadel, D. Maretzki, F.J. Bartl, E. Ritter, K. Palczewski, K.P. Hofmann, Signaling states of rhodopsin. Formation of the storage form, metarhodopsin III, from active metarhodopsin II, J. Biol. Chem. 278 (2003) 3162–3169.

[80] R. Piechnick, E. Ritter, P.W. Hildebrand, O.P. Ernst, P. Scheerer, K.P. Hofmann, M. Heck, Effect of channel mutations on the uptake and release of the retinal ligand in opsin, Proc. Natl. Acad. Sci. U. S. A. 109 (2012) 5247–5252.

[81] M.E. Sommer, W.C. Smith, D.L. Farrens, Dynamics of arrestin–rhodopsin interactions: arrestin and retinal release are directly linked events, J. Biol. Chem. 280 (2005) 6861–6871.

[82] M.H. Chen, C. Kuemmel, R.R. Birge, B.E. Knox, Rapid release of retinal from a cone visual pigment following photoactivation, Biochemistry 51 (2012) 4117–4125.

[83] Y. Imamoto, I. Seki, T. Yamashita, Y. Shichida, Efficiencies of activation of transducin by cone and rod visual pigments, Biochemistry 52 (2013) 3010–3018.

[84] S.A. Schadel, M. Heck, D. Maretzki, S. Filipek, D.C. Teller, K. Palczewski, K.P. Hofmann, Ligand channeling within a G-protein-coupled receptor. The entry and exit of retinals in native opsin, J. Biol. Chem. 278 (2003) 24896–24903.

[85] P.J. Booth, S.L. Flitsch, L.J. Stern, D.A. Greenhalgh, P.S. Kim, H.G. Khorana, Intermediates in the folding of the membrane protein bacteriorhodopsin, Nat. Struct. Biol. 2 (1995) 139–143.

[86] P. Curnow, P.J. Booth, The contribution of a covalently bound cofactor to the folding and thermodynamic stability of an integral membrane protein, J. Mol. Biol. 403 (2010) 630–642.

[87] A. Dutta, K.C. Tirupula, U. Alexiev, J. Klein-Seetharaman, Characterization of membrane protein non-native states. 1. Extent of unfolding and aggregation of rhodopsin in the presence of chemical denaturants, Biochemistry 49 (2010) 6317–6328.

[88] A. Dutta, T.Y. Kim, M. Moeller, J. Wu, U. Alexiev, J. Klein-Seetharaman, Characterization of membrane protein non-native states. 2. The SDS-unfolded states of rhodopsin, Biochemistry 49 (2010) 6329–6340.

[89] R. Renthal, L. Brancaleon, I. Pena, F. Silva, L.Y. Chen, Interaction of a two-transmembrane-helix peptide with lipid bilayers and dodecyl sulfate micelles, Biophys. Chem. 159 (2011) 321–327.

[90] D.J. Jang, M.A. el-Sayed, Tryptophan fluorescence quenching as a monitor for the protein conformation changes occurring during the photocycle of bacteriorhodopsin under different perturbations, Proc. Natl. Acad. Sci. U. S. A. 86 (1989) 5815–5819.

[91] J.M. Janz, D.L. Farrens, Rhodopsin activation exposes a key hydrophobic binding site for the transducin alpha-subunit C terminus, J. Biol. Chem. 279 (2004) 29767–29773.

[92] H. Tsukamoto, D.L. Farrens, M. Koyanagi, A. Terakita, The magnitude of the light-induced conformational change in different rhodopsins correlates with their ability to activate G proteins, J. Biol. Chem. 284 (2009) 20676–20683.

[93] S. Madathil, K. Fahmy, Lipid protein interactions couple protonation to conformation in a conserved cytosolic domain of G protein-coupled receptors, J. Biol. Chem. 284 (2009) 28801–28809.

[94] H. Tsukamoto, A. Sinha, M. DeWitt, D.L. Farrens, Monomeric rhodopsin is the minimal functional unit required for arrestin binding, J. Mol. Biol. 399 (2010) 501–511.

[95] J. Kriegsmann, I. Gregor, I. von der Hocht, J. Klare, M. Engelhard, J. Enderlein, J. Fitter, Translational diffusion and interaction of a photoreceptor and its cognate transducer observed in giant unilamellar vesicles by using dual-focus FCS, ChemBioChem 10 (2009) 1823–1829.

[96] R. Renthal, N. Dawson, J. Tuley, P. Horowitz, Constraints on the flexibility of bacteriorhodopsin's carboxyl-terminal tail at the purple membrane surface, Biochemistry 22 (1983) 5–12.

[97] K. Kirchberg, T.-Y. Kim, S. Haase, U. Alexiev, Functional interaction structures of the photochromic retinal protein rhodopsin, Photochem. Photobiol. Sci. 9 (2010) 226–233.

[98] D.C. Mitchell, B.J. Litman, Effect of ethanol and osmotic stress on receptor conformation. Reduced water activity amplifies the effect of ethanol on metarhodopsin II formation, J. Biol. Chem. 275 (2000) 5355–5360.

[99] S.L. Niu, D.C. Mitchell, Effect of packing density on rhodopsin stability and function in polyunsaturated membranes, Biophys. J. 89 (2005) 1833–1840.

[100] S.E. Mansoor, H.S. McHaourab, D.L. Farrens, Determination of protein secondary structure and solvent accessibility using site-directed fluorescence labeling. Studies of T4 lysozyme using the fluorescent probe monobromobimane, Biochemistry 38 (1999) 16383–16393.

[101] S.E. Mansoor, D.L. Farrens, High-throughput protein structural analysis using site-directed fluorescence labeling and the bimane derivative (2-pyridyl)dithiobimane, Biochemistry 43 (2004) 9426–9438.

[102] J. Klein-Seetharaman, E.V. Getmanova, M.C. Loewen, P.J. Reeves, H.G. Khorana, NMR spectroscopy in studies of light-induced structural changes in mammalian rhodopsin: applicability of solution (19)F NMR, Proc. Natl. Acad. Sci. U. S. A. 96 (1999) 13744–13749.

[103] K. Cai, J. Klein-Seetharaman, J. Hwa, W.L. Hubbell, H.G. Khorana, Structure and function in rhodopsin: effects of disulfide cross-links in the cytoplasmic face of rhodopsin on transducin activation and phosphorylation by rhodopsin kinase, Biochemistry 38 (1999) 12893–12898.

[104] D.L. Farrens, C. Altenbach, K. Yang, W.L. Hubbell, H.G. Khorana, Requirement of rigid-body motion of transmembrane helices for light activation of rhodopsin, Science 274 (1996) 768–770.

[105] S.P. Sheikh, T.A. Zvyaga, O. Lichtarge, T.P. Sakmar, H.R. Bourne, Rhodopsin activation blocked by metal-ion-binding sites linking transmembrane helices C and F, Nature 383 (1996) 347–350.

[106] M. Struthers, H. Yu, D.D. Oprian, G protein-coupled receptor activation: analysis of a highly constrained, "straitjacketed" rhodopsin, Biochemistry 39 (2000) 7938–7942.

[107] N. Radzwill, K. Gerwert, H.J. Steinhoff, Time-resolved detection of transient movement of helices F and G in doubly spin-labeled bacteriorhodopsin, Biophys. J. 80 (2001) 2856–2866.

[108] J. Vonck, A three-dimensional difference map of the N intermediate in the bacteriorhodopsin photocycle: part of the F helix tilts in the M to N transition, Biochemistry 35 (1996) 5870–5878.

[109] S. Subramaniam, M. Gerstein, D. Oesterhelt, R. Henderson, Electron diffraction analysis of structural changes in the photocycle of bacteriorhodopsin, EMBO J. 12 (1993) 1–8.

[110] N.A. Dencher, D. Dresselhaus, G. Zaccai, G. Buldt, Structural changes in bacteriorhodopsin during proton translocation revealed by neutron diffraction, Proc. Natl. Acad. Sci. U. S. A. 86 (1989) 7876–7879.

[111] A.A. Wegener, I. Chizhov, M. Engelhard, H.J. Steinhoff, Time-resolved detection of transient movement of helix F in spin-labelled pharaonis sensory rhodopsin II, J. Mol. Biol. 301 (2000) 881–891.

[112] K.H. Jung, E.N. Spudich, V.D. Trivedi, J.L. Spudich, An archaeal photosignal-transducing module mediates phototaxis in *Escherichia coli*, J. Bacteriol. 183 (2001) 6365–6371.

[113] H. Luecke, B. Schobert, J.K. Lanyi, E.N. Spudich, J.L. Spudich, Crystal structure of sensory rhodopsin II at 2.4 angstroms: insights into color tuning and transducer interaction, Science 293 (2001) 1499–1503.

[114] V.I. Gordeliy, J. Labahn, R. Moukhametzianov, R. Efremov, J. Granzin, R. Schlesinger, G. Buldt, T. Savopol, A.J. Scheidig, J.P. Klare, M. Engelhard, Molecular basis of transmembrane signalling by sensory rhodopsin II-transducer complex, Nature 419 (2002) 484–487.

[115] O.A. Sineshchekov, K.H. Jung, J.L. Spudich, Two rhodopsins mediate phototaxis to low- and high-intensity light in *Chlamydomonas reinhardtii*, Proc. Natl. Acad. Sci. U. S. A. 99 (2002) 8689–8694.

[116] J.L. Spudich, H. Luecke, Sensory rhodopsin II: functional insights from structure, Curr. Opin. Struct. Biol. 12 (2002) 540–546.

[117] X. Yao, C. Parnot, X. Deupi, V.R. Ratnala, G. Swaminath, D. Farrens, B. Kobilka, Coupling ligand structure to specific conformational switches in the beta2-adrenoceptor, Nat. Chem. Biol. 2 (2006) 417–422.

[118] J.F. Fay, D.L. Farrens, A key agonist-induced conformational change in the cannabinoid receptor CB1 is blocked by the allosteric ligand Org 27569, J. Biol. Chem. 287 (2012) 33873–33882.

[119] H.E. Hamm, D. Deretic, A. Arendt, P.A. Hargrave, B. Koenig, K.P. Hofmann, Site of G protein binding to rhodopsin mapped with synthetic peptides from the alpha subunit, Science 241 (1988) 832–835.

[120] E.L. Martin, S. Rens-Domiano, P.J. Schatz, H.E. Hamm, Potent peptide analogues of a G protein receptor-binding region obtained with a combinatorial library, J. Biol. Chem. 271 (1996) 361–366.

[121] O.G. Kisselev, J. Kao, J.W. Ponder, Y.C. Fann, N. Gautam, G.R. Marshall, Light-activated rhodopsin induces structural binding motif in G protein alpha subunit, Proc. Natl. Acad. Sci. U. S. A. 95 (1998) 4270–4275.

[122] D.M. Brabazon, N.G. Abdulaev, J.P. Marino, K.D. Ridge, Evidence for structural changes in carboxyl-terminal peptides of transducin alpha-subunit upon binding a soluble mimic of light-activated rhodopsin, Biochemistry 42 (2003) 302–311.

[123] S. Acharya, Y. Saad, S.S. Karnik, Transducin-alpha C-terminal peptide binding site consists of C–D and E–F loops of rhodopsin, J. Biol. Chem. 272 (1997) 6519–6524.

[124] X. Wang, S.H. Kim, Z. Ablonczy, R.K. Crouch, D.R. Knapp, Probing rhodopsin–transducin interactions by surface modification and mass spectrometry, Biochemistry 43 (2004) 11153–11162.

[125] P. Scheerer, J.H. Park, P.W. Hildebrand, Y.J. Kim, N. Krauss, H.W. Choe, K.P. Hofmann, O.P. Ernst, Crystal structure of opsin in its G-protein-interacting conformation, Nature 455 (2008) 497–502.

[126] R. Herrmann, M. Heck, P. Henklein, P. Henklein, C. Kleuss, K.P. Hofmann, O.P. Ernst, Sequence of interactions in receptor-G protein coupling, J. Biol. Chem. 279 (2004) 24283–24290.

[127] K. Palczewski, T. Kumasaka, T. Hori, C.A. Behnke, H. Motoshima, B.A. Fox, I. Le Trong, D.C. Teller, T. Okada, R.E. Stenkamp, M. Yamamoto, M. Miyano, Crystal structure of rhodopsin: A G protein-coupled receptor, Science 289 (2000) 739–745.

[128] V.V. Gurevich, J.L. Benovic, Visual arrestin binding to rhodopsin. Diverse functional roles of positively charged residues within the phosphorylation-recognition region of arrestin, J. Biol. Chem. 270 (1995) 6010–6016.

[129] H. Kuhn, Light-regulated binding of proteins to photoreceptor membranes and its use for the purification of several rod cell proteins, Methods Enzymol. 81 (1982) 556–564.

[130] A. Mendez, M.E. Burns, A. Roca, J. Lem, L.W. Wu, M.I. Simon, D.A. Baylor, J. Chen, Rapid and reproducible deactivation of rhodopsin requires multiple phosphorylation sites, Neuron 28 (2000) 153–164.

[131] S.K. Gibson, J.H. Parkes, P.A. Liebman, Phosphorylation modulates the affinity of light-activated rhodopsin for G protein and arrestin, Biochemistry 39 (2000) 5738–5749.

[132] R.D. Hamer, S.C. Nicholas, D. Tranchina, P.A. Liebman, T.D. Lamb, Multiple steps of phosphorylation of activated rhodopsin can account for the reproducibility of vertebrate rod single-photon responses, J. Gen. Physiol. 122 (2003) 419–444.

[133] W.C. Smith, A. Dinculescu, J.J. Peterson, J.H. McDowell, The surface of visual arrestin that binds to rhodopsin, Mol. Vis. 10 (2004) 392–398.

[134] M.E. Sommer, D.L. Farrens, Arrestin can act as a regulator of rhodopsin photochemistry, Vision Res. 46 (2006) 4532–4546.

[135] D. Fotiadis, Y. Liang, S. Filipek, D.A. Saperstein, A. Engel, K. Palczewski, Atomic-force microscopy: rhodopsin dimers in native disc membranes, Nature 421 (2003) 127–128.

[136] T.H. Bayburt, S.A. Vishnivetskiy, M.A. McLean, T. Morizumi, C.C. Huang, J.J. Tesmer, O.P. Ernst, S.G. Sligar, V.V. Gurevich, Monomeric rhodopsin is sufficient for normal rhodopsin kinase (GRK1) phosphorylation and arrestin-1 binding, J. Biol. Chem. 286 (2011) 1420–1428.

[137] T.H. Bayburt, A.J. Leitz, G. Xie, D.D. Oprian, S.G. Sligar, Transducin activation by nanoscale lipid bilayers containing one and two rhodopsins, J. Biol. Chem. 282 (2007) 14875–14881.

[138] S. Banerjee, T. Huber, T.P. Sakmar, Rapid incorporation of functional rhodopsin into nanoscale apolipoprotein bound bilayer (NABB) particles, J. Mol. Biol. 377 (2008) 1067–1081.

[139] M.R. Whorton, B. Jastrzebska, P.S. Park, D. Fotiadis, A. Engel, K. Palczewski, R.K. Sunahara, Efficient coupling of transducin to monomeric rhodopsin in a phospholipid bilayer, J. Biol. Chem. 283 (2008) 4387–4394.

[140] P.S. Park, S. Filipek, J.W. Wells, K. Palczewski, Oligomerization of G protein-coupled receptors: past, present, and future, Biochemistry 43 (2004) 15643–15656.

[141] V.V. Gurevich, E.V. Gurevich, GPCR monomers and oligomers: it takes all kinds, Trends Neurosci. 31 (2008) 74–81.

[142] M.E. Sommer, K.P. Hofmann, M. Heck, Arrestin-rhodopsin binding stoichiometry in isolated rod outer segment membranes depends on the percentage of activated receptors, J. Biol. Chem. 286 (2011) 7359–7369.

[143] M.E. Sommer, K.P. Hofmann, M. Heck, Distinct loops in arrestin differentially regulate ligand binding within the GPCR opsin, Nat. Commun. 3 (2012) 995.

[144] H. Tsukamoto, I. Szundi, J.W. Lewis, D.L. Farrens, D.S. Kliger, Rhodopsin in nanodiscs has native membrane-like photointermediates, Biochemistry 50 (2011) 5086–5091.

[145] H. Tsukamoto, D.L. Farrens, A constitutively activating mutation alters the dynamics and energetics of a key conformational change in a ligand-free G protein-coupled receptor, J. Biol. Chem. 288 (2013) 28207–28216.

[146] T. Huber, T.P. Sakmar, Escaping the flatlands: new approaches for studying the dynamic assembly and activation of GPCR signaling complexes, Trends Pharmacol. Sci. 32 (2011) 410–419.

[147] A.M. Knepp, T.P. Sakmar, T. Huber, Homogeneous time-resolved fluorescence assay to probe folded G protein-coupled receptors, Methods Enzymol. 522 (2013) 169–189.